Impact of Climate Change on Weather Related Fire Risk in the Tasmanian Wilderness World Heritage Area

Peter Love, Paul Fox-Hughes, Tom Remenyi, Rebecca Harris, Nathan Bindoff

Tasmanian Wilderness World Heritage Area Climate Change and Bushfire Research Initiative

Citation

Love, P. T., Fox-Hughes, P., Remenyi, T. A., Harris, R. M. B., Bindoff N. L. (2017), Impact of climate change on weather related fire risk in the Tasmanian Wilderness World Heritage Area Climate Change and Bushfire Research Initiative, Technical Report, Antarctic Climate and Ecosystems Cooperative Research Centre, Hobart, Tasmania.

Summary

Implications for Tasmanian Wilderness World Heritage Area Management

The Tasmanian Wilderness World Heritage Area Management (TWWHA) has been recognised for its outstanding universal values, with many of these values being dependent on specific fire regimes for their maintenance. For example, the highly fire sensitive palaeoendemics such as king-billy pine, pencil pine, huon pine and deciduous beech may be destroyed by a single fire, while in contrast, buttongrass moorlands and native grasslands may be lost if the period between fires is too long.

Climate Futures for Tasmania data indicates that climate change is highly likely to result in profound changes to the fire regime of the TWWHA, which therefore, has profound implications for values and management of the TWWHA.

The most significant factor which has the potential to impact on the values and fire management of the TWWHA is the projected very large increase in dryness. This increase in dryness is reflected in the increases in the Mount Soil Dryness Index (MSDI), the number of days in a season when the MSDI exceeds the critical threshold of 50 and the number of times in a season when there are greater than 30 days with less than 50 mm of precipitation.

In summer, these enhanced levels of dryness will mean that when bushfires occur (from whatever cause) the potential for the fires to burn into organic soils, rainforest and alpine areas will be greatly increased. In addition, by 2100 conditions typical of summer are projected to be about eight weeks longer. These changes are projected to start occurring in the near-future time period (ie 2010 to 2030) and get progressively worse by 2100.

The window within which planned burning can be reliably conducted will be greatly reduced. This will be due to spring being reduced in length by about two weeks and autumn by about six weeks. In addition, mean wind speeds are projected to significantly increase in spring (but less so in autumn and summer), further restricting the potential for planned burning. This will mean that by 2100 the number of days per season suitable for planned burning in the TWWHA will be reduced by about half.

The occurrence of dry lightning is projected to steadily decrease, however, it is likely that this will be more than offset by the very substantial increases in soil and fuel dryness. In addition, large outbreaks of dry lightning are projected to occur earlier in the season. As a result, the widespread fires ignited by these events are likely to be present in the landscape for more of the season leading to larger fire affected areas.

The increased potential for summer bushfires that result from the enhanced dryness has the potential to reverse the marked reduction in arson, accidental fires, and escaped management burns that have occurred in the TWWHA between the 1970s and 2010s. In doing so, it is possible this increase in fire potential will result in a return to the situation that prevailed over the 100 years prior to the 1970s when catastrophic impacts to fire sensitive paleoendemics occurred. These impacts included the destruction of about 30 to 50 % of king-billy pine, more than 50 % of pencil pine forest, and 10 % of huon pine, along with extensive areas of deciduous beech and organic soils.

Technical Summary

Climate Futures for Tasmania (CFT) dynamically downscaled Tasmanian regional climate projections have been analysed to assess future changes to weather related fire risk in the TWWHA and influential adjacent reserves and vegetation westward of the TWWHA (Adjacent Areas).

This work builds on the CFT Future Fire Danger Project, in which it was found that fire danger as measured by the McArthur Forest Fire Danger Index (FFDI) was projected to increase across the state. While the absolute increase in FFDI in western Tasmania was smaller, the relative increase over current levels was larger. In the present study this result is found to be consistent in the TWWHA with even stronger increases in the Adjacent Areas.

The main driver of FFDI is the Mount Soil Dryness Index (MSDI), a metric which has been linked to fire danger in a range of vegetation and soil types occuring in the TWWHA. Large increases in MSDI are projected, accelerating towards the end of the century. On the basis of this measure, the observed trend in recent decades of steadily increasing fire danger during spring is projected to continue throughout the current century, while autumn fire danger will begin to increase in the near future. By the end of the century, summer conditions are projected to persist around eight weeks longer at the expense of shorter autumn and spring conditions.

During the fire season (October-March) in the TWWHA the average MSDI exceeds 75 once every six years (99.9th percentile) throughout the historical period up to the present. This is projected to increase to twice each fire season by mid-century (99th percentile) and to 9 days each fire season (95th percentile) by the end of the century.

The effect of decreasing wind speed on fire danger in buttongrass moorlands is offset by significant decreases in dead-fuel moisture leading to slight increases in mean Buttongrass Moorland Fire Danger Index (MFDI). The

summer peak of extreme MFDI decreases while a secondary peak in autumn strengthens slightly to become dominant.

In the Adjacent Areas the patterns in these fire danger indices is similar, however, while the values are slightly lower, the percentage increases are higher.

Threshold values of *MSDI > 50* and *30-day total rainfall less than 50 mm* have both been shown to be predictors for fire in Tasmanian rainforests. The occurrence of these conditions is projected to increase significantly. The number of days per fire season that MSDI > 50 at any given location in the TWWHA is projected to triple by the end of the century. For the occurrence of the 30-day dry periods this number is projected to double. In the Adjacent Areas these indicators show a very dramatic change in conditions with mean daily extent of affected area increasing from near zero percent to around 10% for MSDI > 50, and 6% for dry periods.

Lightning outbreaks in general decrease in extent and frequency, although not necessarily intensity, as a result of increasing stability. The decrease in the extent of the largest outbreaks at the summer peak is small although the duration of summer Dry Lightning Potential Environment (DLPE) conditions becomes much shorter. The timing of the summer peak shifts to earlier in the season. The significant increase in lightning fire affected areas recorded over recent years suggests that the decrease in lightning outbreaks is being offset by the dramatic increases in dryness, so that when lightning does occur fires are much more likely to be sustained.

No strong trends are projected in the frequency with which synoptic patterns occur on an annual basis. In summer and to some extent in autumn, there is evidence of an increase in weather patterns favouring easterly winds, and a decrease in strong northwesterly to southwesterly streams. These changes explain, at least partially, the projected increase in MSDI.

Contents

List of Acronyms

ACE CRC	Antarctic Climate and Ecosystems Cooperative Research Centre
CCAM	Conformal Cubic Atmospheric Model
CMIP3	Coupled Model Intercomparison Project phase 3
CFT	Climate Futures for Tasmania
DF	Drought Factor
DLPE	Dry Lightning Potential Environment
ENSO	El Niño–Southern Oscillation
FFDI	Forest Fire Danger Index
GCM	General Circulation Model
IOD	Indian Ocean Dipole
IPCC	Intergovernmental Panel on Climate Change
MF	Moisture Factor
MFDI	Moorland Fire Danger Index
MJO	Madden-Julian Oscillation
MMM	Multi-model-mean
MSDI	Mount Soil Dryness Index
SAM	Southern Annular Mode
SRES	Special Report on Emissions Scenarios
TWWHA	Tasmanian Wilderness World Heritage Area
TBCCRP	TWWHA Bushfire and Climate Change Research Project

1 Introduction

During 2015 western Tasmania experienced the driest spring on record. Combined with record high spring maximum temperatures, this created high fire danger conditions which persisted throughout the summer of 2015-16. This summer was the warmest Tasmanian summer on record with below average rainfall in the west and south [*Jones et al.*, 2009].

Intense lightning storms in January and February 2016 ignited fires across the state. More than 200 vegetation fires were recorded during the first three months of the year. These fires burned more than 125,000 hectares and required significant resources to observe and control [*AFAC*, 2016]. The cost to the state was more than $50 million [*Press*, 2016]. Nearly 20,000 hectares of the affected areas were within the Tasmanian Wilderness World Heritage Area (TWWHA), a small portion of which comprised fire-sensitive alpine and sub-alpine vegetation types which characterise the TWWHA's natural Outstanding Universal Value [*AFAC*, 2016]. These fire-sensitive vegetation types are typically only susceptible to fire during very dry conditions, such as were experienced during this period.

Recognising the potential for such conditions to occur more frequently as a result of anthropogenic climate change, the Tasmanian Government initiated the TWWHA Bushfire and Climate Change Research Project (TBCCRP) [*Press*, 2016]. The research described in the present report was commissioned as part of the TBCCRP and builds on the Climate Futures for Tasmania (CFT) Future Fire Danger Project conducted previously by the Antarctic Climate and Ecosystems Cooperative Research Centre (ACE CRC) [*Fox-Hughes et al.*, 2015]. Although the main focus was the TWWHA, it was recognised that there were influential adjacent reserves and vegetation westward of the TWWHA (hereafter Adjacent Areas) that were of relevance to managers. Therefore for this study there are two major regions analysed (Figure 1.1).

Since the initiation of the TBCCRP several independent studies have been conducted to investigate the role of anthropogenic climate change in causing the extreme weather patterns associated with the January–March 2016 Tasmanian bushfires. *Hope et al.* [2016] noted that various large-scale patterns of climate variability were in a state favourable for warm dry weather in southern Australia during spring 2015, including the Indian Ocean Dipole (IOD), the Madden-Julian Oscillation (MJO), the Southern Annular Mode (SAM), blocking in the Tasman Sea and a particularly strong El Niño. *Karoly et al.* [2016] found that the presence of the strong El Niño was a significant factor increasing the likelihood of record low rainfall during October 2015, and additionally that it was very likely that anthropogenic climate change
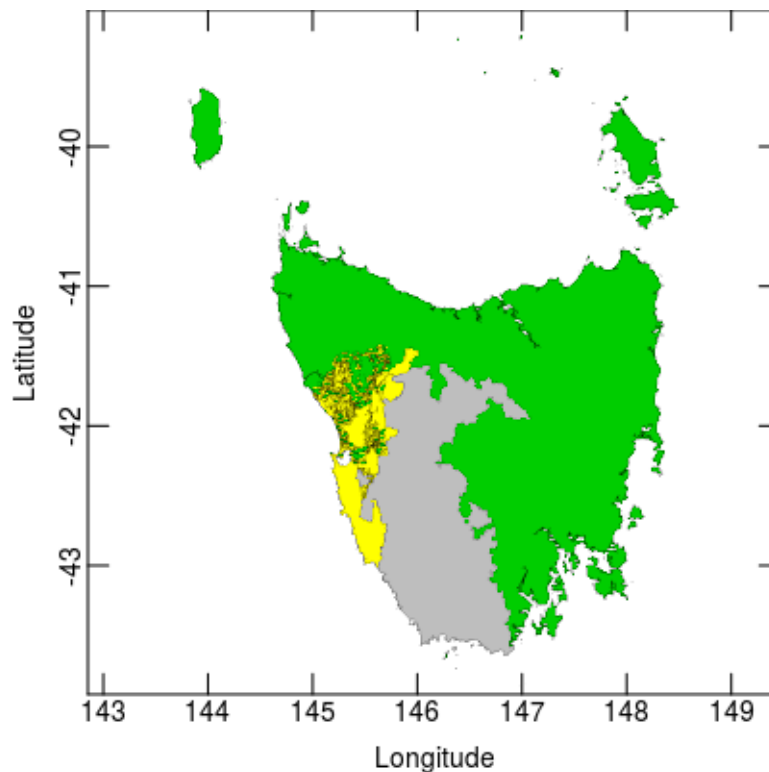
Figure 1.1: Boundaries of the Tasmanian Wilderness World Heritage Area (TWWHA) (grey) and the influential adjacent reserves and vegetation westward of the TWWHA (yellow).

increased this likelihood.

With respect to record breaking temperatures, *Black and Karoly* [2016] concluded that the particularly strong El Niño did not play a significant role in the October 2015 event. This conclusion was also reached using different methods by *Hope et al.* [2016], who also found that the combined state of intraseasonal atmospheric drivers such as the MJO, the negative SAM and Tasman Sea blocking did make a contribution to increasing likelihood of this event. *Black and Karoly* [2016] found it was very likely that anthropogenic climate change increased the likelihood of record breaking temperatures by 400%, a finding that was supported by *Hope et al.* [2016].

To assess the future impact of anthropogenic climate change on the weather-related fire risk within the TWWHA this study utilised the CFT regional climate projections [*Corney et al.*, 2010]. The CFT projections were generated using the Conformal Cubic Atmospheric Model (CCAM) to dynamically downscale the output of six general circulation models (GCMs) from the Cou-

pled Model Intercomparison Project phase 3 (CMIP3) archive. Projections based on the IPCC SRES A2 high emissions scenario, which has been consistent with recent observed CO_2 emissions, are used in the present study. The output of the downscaling process provided gridded data for a range of meteorological parameters at 10 km horizontal resolution across Tasmania for the period of 1961–2100.

The CFT Future Fire Danger project [*Fox-Hughes et al.*, 2015] used these gridded data to produce statewide daily estimates of the McArthur Forest Fire Danger Index (FFDI). The projections of FFDI were validated against observational data for the historical period. Regional patterns in static decadal average (2002–2012) FFDI were shown to be consistent with observations, indicating that the simulations represent the current climate well. Additionally, the observed increase in spring fire danger, together with very little change in autumn fire danger [*Fox-Hughes*, 2008], are captured well by the models [*Fox-Hughes et al.*, 2014]. The ability of the models to reproduce recent observed climate change provides confidence that they can provide accurate projections into the future.

These data were used to calculate daily estimates of fire danger indices and fuel dryness indicators. Statistical analysis of the projected changes to mean conditions and extreme occurrences of these indices are described in Section 2. This analysis is extended in Section 3 to examine threshold values of these indices that have been identified as predictors of fire in Tasmanian rainforest. Similar analysis of estimates of the likelihood of occurrence of dry lightning is presented in Section 4. Projected changes to the frequency of typical synoptic weather patterns over Tasmania are discussed in Section 5.

Further statistical analysis of these fire danger, dryness and lightning potential indices, and additional meteorological parameters, has been carried out to produce another two deliverables. Statistics for each calendar month have been calculated on a decadal basis across all Bureau of Meteorology Tasmanian weather station areas of influence and provided to the Tasmanian Parks and Wildlife Service in shapefile format. A description of these data and access details are given in Appendix E. Gridded statistics were also calculated for the same parameters within the TWWHA for four 20-year sub-periods and provided to Dr Jonathan Marsden-Smedley for application in his research on historical lightning fires that was also commisioned as part of the TBCCRP. A description of these data and access details are given in Appendix F.

2   Fire Danger Indices

2.1   Analysis Methods

The statistics of the FFDI data produced by the CFT Future Fire Danger project have been analysed here using methods similar to those described in *Fox-Hughes et al.* [2014] for the regions of the TWWHA and Adjacent Areas. For each grid cell within the two regions of interest, the 80th, 90th and 99th percentile, and mean FFDI values, were calculated for each year of the CFT period and for each of the six models. These statistics were calculated for both the bushfire season (October–March) and for the full year (July–June). Multi-model-means (MMM) of these statistics were calculated for each grid cell. Mean values of each statistic were then calculated across the two regions.

In addition to the yearly values, the statistics were calculated over four 20-year sub-periods; baseline (1980-2000), near-future (2010-2030), mid-century (2040-2060) and end-of-century (2080-2100). This resulted in more robust estimates of higher percentiles, with values calculated for the 85th, 90th, 95th, 99th, 99.5th and 99.9th percentiles.

The projected seasonal evolution of the mean and percentile statistics was examined using similar methods to the 20-year analysis. The statistics were calculated for each calendar month within 30-year windows stepped forward at 1-year intervals through the full CFT period. Thus, for each calendar month a time-series of each percentile was obtained spanning the 140 years of the CFT period. The annual cycle of each statistic could then be assessed at any point throughout the CFT period and changes to the seasonality noted.

The same methods were applied to the Buttongrass Moorland Fire Danger Index (MFDI) and the Mount Soil Dryness Index (MSDI).

2.2   McArthur Forest Fire Danger Index

The McArthur Forest Fire Danger Index (FFDI) [*McArthur*, 1967; *Noble et al.*, 1980] is a standard index used by weather forecasters and fire services in eastern Australia to determine fire hazard and make operational decisions around fire management. The FFDI incorporates surface air temperature, relative humidity and wind speed, combined with an estimate of fuel dryness (Drought Factor, based on soil moisture deficit and recent precipitation) to give an index of daily fire danger. The index is based on dry eucalypt forest fire behaviour measurements.

The projected MMM regional fire season mean FFDI for the TWWHA is plotted in Figure 2.1. Crosses indicate values of the fire season mean FFDI for each year in the CFT period averaged across all grid cells in the TWWHA.

While the annual values exhibit large interannual variability, there is a clear increasing trend. A 30-year running mean was applied to the annual values (black line) to smooth the interannual variability and highlight the trend, which accelerates towards the end of the century. Grey shading indicates the spread of the projections determined from the six CMIP3 models. These results are consistent with the analysis of the Western region of *Fox-Hughes et al.* [2014].
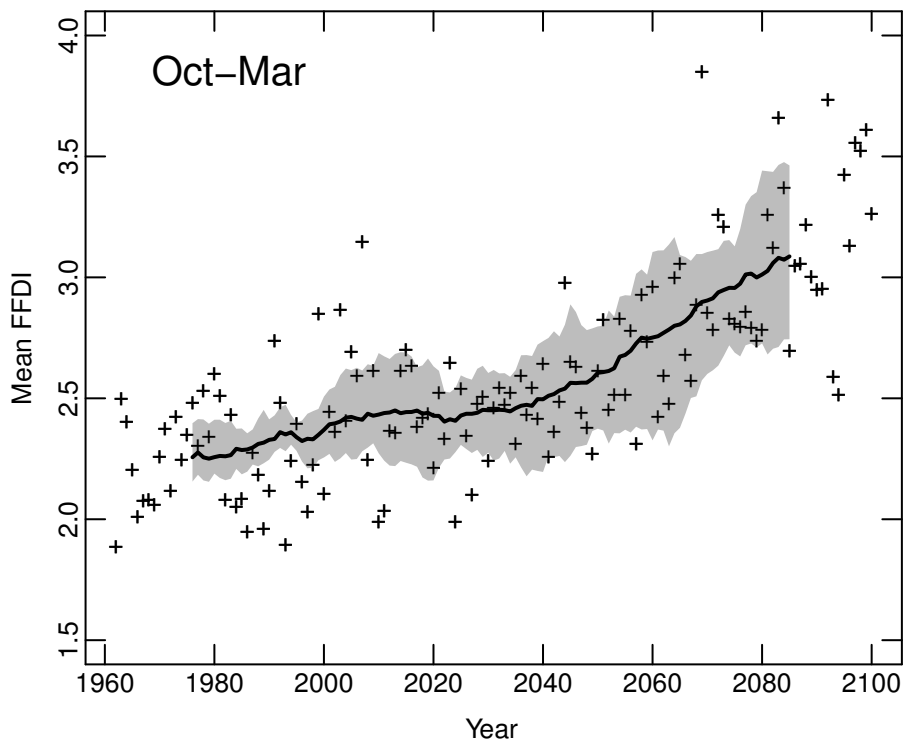
Figure 2.1: Projected multi-model mean regional fire season mean (October-March) forest fire danger index for the TWWHA. Annual fire season mean (crosses) and 30-year running mean (black line). Grey shading indicates the spread of the projections determined from the six individual models.

A very similar trend is observed in all of the FFDI statistics calculated over the fire season and additionally when calculated over the full year. The same trend is also observed in the FFDI statistics for the Adjacent Areas. The trend is quantified in the analysis of the four 20-year sub-periods, summarised in Table A-1 in Appendix A, where the statistics for each sub-period are given together with the percentage increase over the baseline period. For example, in the TWWHA during the baseline period, the 99.5th percentile TWWHA

averaged fire season FFDI is 21.83. This means that during this period it is expected that there will be approximately one day per fire season when the average FFDI within the TWWHA will be 21.83 or higher. By the end-of-century period the 99.5th percentile has increased to 26.74, which represents a 22.5% increase over the value for the baseline period.

The increase in the FFDI on the most extreme days during the fire season is 11% by mid-century and 21% by end-of-century. This trend becomes steadily stronger towards the lower percentiles to around 14% and 40% for the 85th percentile at the mid- and end-of-century periods respectively. Statistics for the full year have smaller absolute values but show similar percentage increases. In the Adjacent Areas FFDI is consistently lower than the TWWHA, however, the percentage increases are all significantly larger. By the end-of-century period fire season mean FFDI increases by 37.5% in the TWWHA and by 49.2% in the Adjacent Areas.

The 99th percentile FFDI calculated over 30-year windows for each month have been plotted in Figure 2.2 as a function of year of CFT period (horizontal axis) and calendar month (vertical axis). The tendency in the seasonality of FFDI is towards a somewhat shorter duration of typical winter conditions, with a slightly longer but more intense summer, peaking in January, and more rapid transitions between winter and summer conditions during autumn. This pattern is consistent across all of the percentiles calculated. Similar plots for each of the percentiles are given for comparison in Figure B-1 in Appendix B.

2.3   Buttongrass Moorland Fire Danger Index

The McArthur Forest Fire Danger Index is known to perform poorly in certain vegetation types, including buttongrass moorlands which cover around 15% of Tasmania [*Marsden-Smedley and Catchpole*, 1995]. A fire behaviour prediction system was developed in the 1990s for buttongrass moorlands. This includes the Buttongrass Moorland Fire Danger Index (MFDI) [*Marsden-Smedley et al.*, 1999] and now forms the basis of operational practice for all buttongrass vegetation in Tasmania. As the majority of Tasmanian buttongrass moorlands are found within the TWWHA, projections of MFDI have been calculated and are described in this section.

Annual fire season mean and 99th percentile MFDI for the TWWHA are plotted in Figure 2.3. Note that the scales on the vertical axes differ in these plots and in subsequent figures. Mean MFDI is projected to increase through the century subject to considerable interannual and interdecadal variability. The percentage increase over the baseline period by the end-of-century is around 6% (Table A-2, Appendix B). In contrast, the 99th percentile exhibits
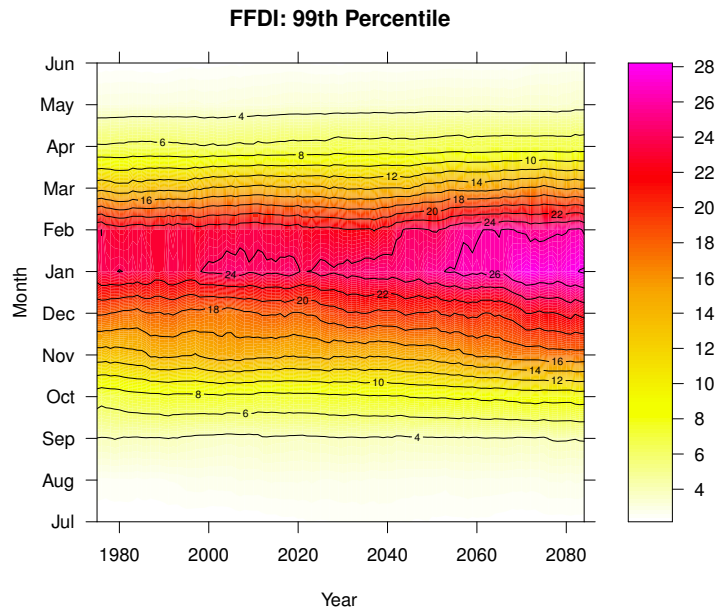
Figure 2.2: Projected multi-model mean regional mean 99th percentile forest fire danger index for the TWWHA, calculated for each calendar month in 30-year windows stepped at 1-year intervals through the period of 1961-2100.

a slight decrease in the MMM, although considering the spread of the models, this trend is not robust. The small percentage decreases of the 99th and higher percentiles in Table A-2 are not statistically significant.

The MFDI statistics for the Adjacent Areas show slightly lower absolute values with similar trends as in the TWWHA. Statistics for the full year in both areas are somewhat smaller than for fire season, again with similar trends.

The two factors contributing to the MFDI are wind speed and buttongrass moorlands dead-fuel Moisture Factor (MF), the latter largely dependent on rainfall during the preceding two days. Mean and 99th percentiles for these parameters are plotted in Figure 2.4. Wind is projected to decrease in general during the fire season. Decreasing wind would drive a decrease in MFDI but is offset by large decreases in MF. The intensity of the windiest days is not projected to change significantly and together with decreasing extremes of MF would seem to imply increasing extremes of MFDI, however, the projected slight decrease in the higher percentiles of MFDI reflects the fact that MFDI captures the coincidence of the two factors as this coincidence is less likely for the higher percentiles if the two parameters are independent.

7
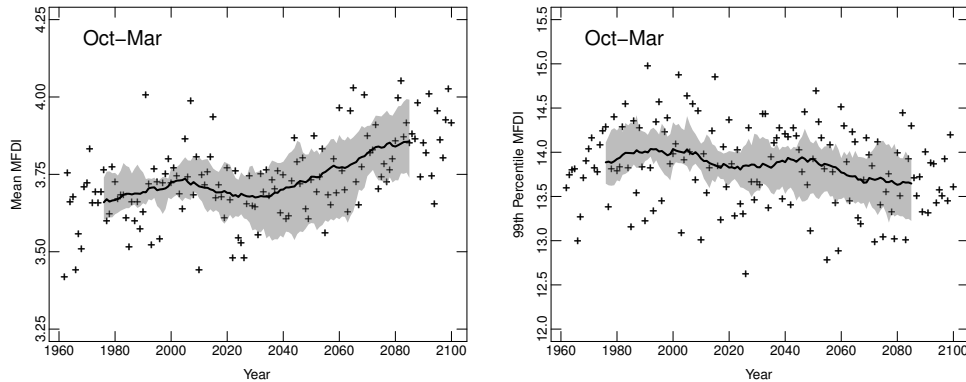
Figure 2.3: Projected mujlti-model mean regional fire season mean (October-March)(left) and 99th percentile (right) moorland fire danger index for the TWWHA. Annual fire season mean and annual fire season 99th percentile are plotted as crosses. Black lines are 30-year running means and grey shading indicates range of 30-year running means of the individual models.

MFDI differs significantly in seasonality from FFDI. The annual variation in MFDI is much smaller, peaking in February for the lower percentiles (Figure 2.5 (left)) while the higher percentiles (Figure 2.5 (right)) show that the most extreme events occur during two peak periods of January–February and October. The slight increase in fire season MFDI for the lower percentiles can be attributed to an earlier start to the summer peak. At the higher percentiles the February peak weakens throughout the CFT period while the October peak strengthens slightly and takes over as the dominant moorland fire danger period.

2.4   Mount Soil Dryness Index

Mount Soil Dryness Index (MSDI) [*Mount*, 1972] was also calculated and analysed across Tasmania for CFT Future Fire Danger Project. It is widely used in predicting vegetation and soil flammability in a range of different environments. In particular, in several recent studies it has been related quantitatively to the flammability of the vegetation and soil types occurring within the TWWHA, although there remains ambiguity in its application to highland and alpine areas.

Very large increases in Mount Soil Dryness Index (MSDI) are projected across all statistics calculated. The projection of the 99th percentile MSDI shown for example in Figure 2.6 is representative of the trend in all of the MSDI statistics across both the TWWHA and Adjacent Areas. Significant

8
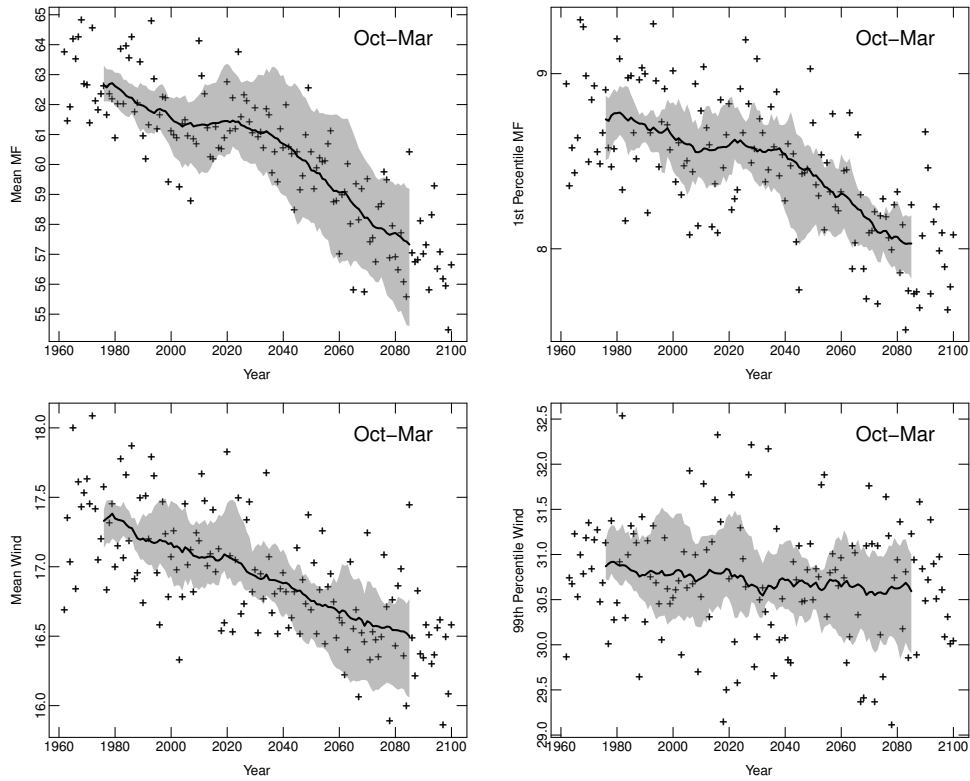
Figure 2.4: Projected multi-model mean regional fire season mean moisture factor (MF) (top left), 1st percentile MF (top right), mean wind speed (km/hour) (bottom left) and 99th percentile wind speed (bottom) for the TWWHA. Annual fire season mean and annual fire season 99th percentile are plotted as crosses. Black lines are 30-year running means and grey shading indicates range of 30-year running means of the individual models.

increases of around 10% in broad indicators are evident in the near future and large increases across all statistics are present by mid-century. From Table A-3 it can be seen that by the end-of-century increases range from close to 50% for the 99.9th percentile to greater than 80% in the mean.

In terms of the frequency of occurrence of high MSDI, Table A-3 shows, for example, that TWWHA average MSDI greater than 75 occurs less than once every six years (99.9th percentile) during the historical and near future periods. By mid-century this is projected to increase to twice each fire season (99th percentile) and to 9 days each fire season (95th percentile) by the end of the century.

As with the FFDI, absolute values of the statistics in the Adjacent Areas are somewhat lower than the TWWHA, however, the percentage increases
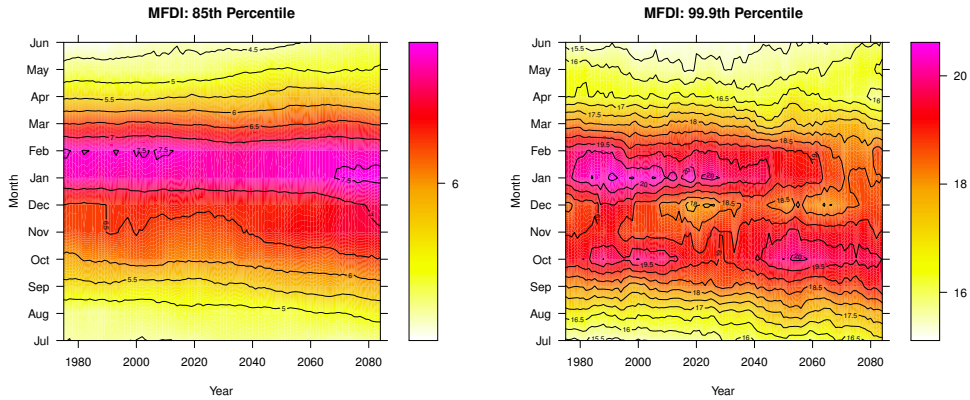
Figure 2.5: Projected multi-model mean regional mean 85th (left) and 99.9th (right) percentile moorland fire danger index, calculated for each calendar month in 30-year windows stepped at 1-year intervals through the period of 1961-2100.

are significantly larger.

The tendency in MSDI seasonality is similar to that of FFDI but more pronounced (Figure 2.7). The shortening of winter conditions is more obvious and the increase in the intensity of extreme events during summer significantly higher.

2.5   Summary

The observed trend of steadily increasing fire danger during spring [*Fox-Hughes*, 2008] is projected to continue throughout the current century. For MSDI this brings the onset of historical spring conditions forward by at least two weeks by the end of the century, while the onset of summer is more than one month earlier. In the near future there is a projected break from the historically steady autumn conditions towards increasing fire danger. By 2100 historical autumn conditions begin around six weeks later than currently and persist for less than two months. As a result summer would be around 8 weeks longer with percentage increases in the summer peak percentiles of 50–100%.

MSDI appears to be the dominant driver of FFDI which exhibits similar although less pronounced changes in seasonality and peak summer percentiles.

Similar decreases in MF are largely offset by decreases in wind speed resulting in relatively small increases in fire season mean MFDI. At the higher percentiles the summer peak weakens throughout the century while the spring

10
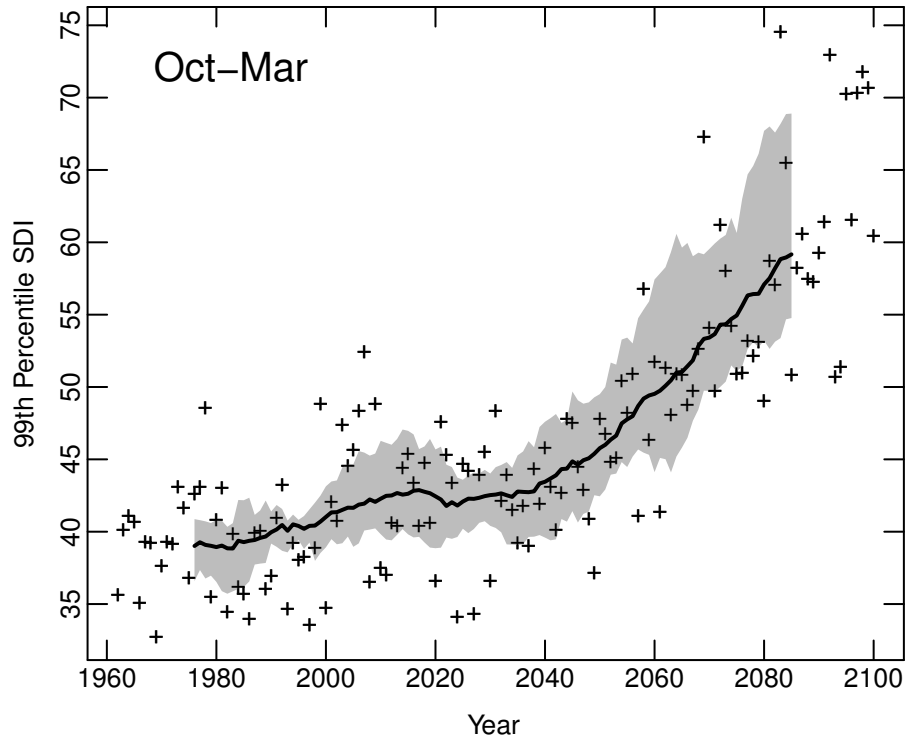
Figure 2.6: Projected moorland fire danger index regional fire season mean (October-March) Mount soil dryness index for the TWWHA. Annual fire season 99th percentile (crosses) and 30-year running mean (black line). Grey shading indicates range of 30-year running means of the individual models.

peak strengthens slightly and takes over as the dominant moorland fire danger period.
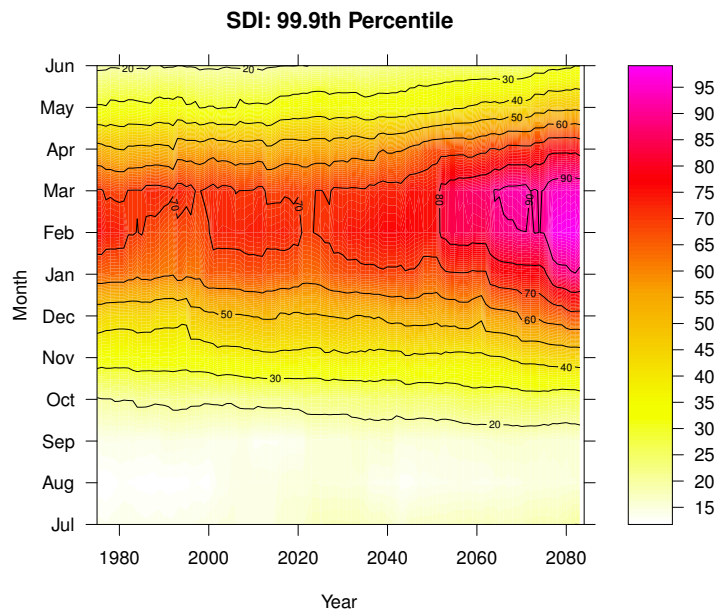
Figure 2.7: Projected multi-model mean regional mean 99.9th percentile Mount soil dryness index, calculated for each calendar month in 30-year windows stepped at 1-year intervals through the period of 1961-2100.

3 Dryness Thresholds

3.1 Analysis Methods

As noted in Section 2.4, MSDI has been related to the flammability of the vegetation and soil types within the TWWHA. In particular, *Marsden-Smedley* [2009] identified the MSDI value of 50 as a significant threshold above which the danger of fire within rainforests was high. *Styger and Kirkpatrick* [2015] found that the occurence of rainfall less than a threshold of 50 mm during the preceding 30 days was a stronger predictor of rainforest fire.

To assess the projected changes to fire danger in rainforests within the TWWHA these threshold values have been analysed in the CFT projections by two methods. First, the total number of days on which each criterion is met was calculated for each grid cell within the TWWHA during each of the four 20-year sub-periods. These totals were then averaged over both the TWWHA and the Adjacent Areas to give the region average "count", expressed as the number of days per fire season or per full year.

Second, the total number of grid cells within each region in which each criterion was met was determined for each day during each sub-period. The mean and various percentiles were then calculated from the time-series of these daily totals, expressed as the areal extent as a percentage of the total area of the either the TWWHA or Adjacent Areas where each threshold criterion was met. This method was also applied on a monthly basis using the 30-year sliding window approach described in Section 2.1, in order to assess changes to the seasonality of these dryness indicators.

3.2 MSDI Threshold

The MSDI threshold count, mean and percentile statistics are given in Table A-5 in Appendix A. All of the statistics for the MSDI threshold are projected to increase very dramatically, although the increase in the highest percentiles is not seen until mid-century. The number of days on which MSDI exceeds 50, averaged over the TWWHA, increases by 16% in the near future, 58% by mid-century and 218% by end-of-century, more than triple the baseline period. The area of the TWWHA, as a percentage, over which MSDI exceeds 50 on a given day is projected to increase equally dramatically. The 95th percentile increases from 22% of the TWWHA to 72% of the TWWHA by end-of-century. Similarly large absolute increases in the areal extent of MSDI greater than 50 are seen for the other percentiles, and similar percentage increases are seen in the mean area. The percentage increase in the higher percentiles is lower as the areal extents above the threshold approach 100% of the TWWHA towards the end of the century.

In the Adjacent Areas the occurrence of MSDI greater than 50 is typically negligible during the baseline period, although the 99th and higher percentiles indicate that the most extreme events do affect a significant areal extent. However, extremely large percentage increases in the count, mean and lower percentiles indicate that this region is projected to experience a significant change toward much drier typical conditions during fire season. By end-of-century 10% of the Adjacent Areas are projected to be subject to MSDI greater than 50 at any given time during fire season compared to around 1% during the baseline period. At any given location in the Adjacent Areas the expected number of days per fire season that are subject to the threshold conditions is projected to increase from 2.6 to 19.5.

Changes to the seasonality of the occurrence of the MSDI threshold are very similar to those seen for MSDI (Figure 2.7) as seen in Figure 3.1, noting however, that the values in Figure 3.1 are percentages of the area within the TWWHA subject to the threshold rather than explicit MSDI. Plots for the other percentiles given in Figure B-4 in Appendix B show very similar characteristics.

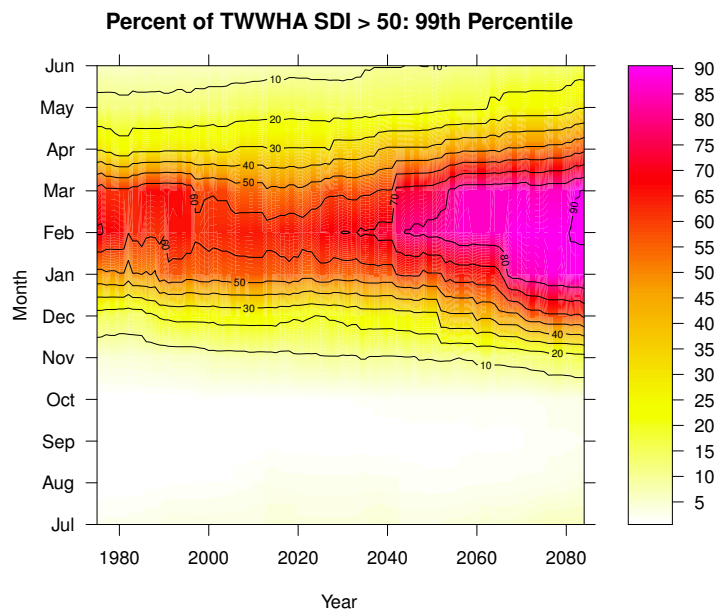**Percent of TWWHA SDI > 50: 99th Percentile**

Figure 3.1: Multi-model mean projection of 99th percentile of area within TWWHA subject to Mount soil dryness index > 50, calculated for each calendar month in 30-year windows stepped at 1-year intervals through the period of 1961-2100.

14

3.3 30-Day Antecedent Rainfall Threshold

The occurrence of days on which the 30-day antecedent rainfall is less than 50 mm is also projected to increase dramatically by the end-of-century period (Table A-6, Appendix A). As with the other parameters considered, the increase accelerates towards the end of the century. The number of days this criterion is met is projected to increase incrementally during the near and mid-century periods and nearly double during fire season by the end of the century. Similar or larger percentage increases are projected for the statistics of the areal extent of this criterion, except at larger percentiles where coverage of the TWWHA during the baseline period is already close to 100%.

Similar to the MSDI threshold, the 30-day dry period statistics in the Adjacent Areas indicate that the region is projected to undergo a significant change in the dryness of typical fire season conditions. There is considerable disparity in the distribution of dry outbreaks in the Adjacent Areas during the baseline period. That is to say, the majority of the time there is no area within the Adjacent Areas subject to a dry period, but when dry periods do occur they are typically widespread through the region. This disparity is projected to decrease leading to more common smaller dry outbreaks in addition to larger extreme events.

The seasonal evolution of the 95th percentile dry period occurrence is shown in Figure 3.2. This also shows the strong increase in areal extent of the largest events during summer, peaking in February–March. Only a very subtle increase in the duration of summer is seen, leading again to more rapid transitions between summer and winter conditions. Plots for other percentiles are given in Figure B-5 in Appendix B. At higher percentiles, as noted above, the summer peak values are already close to 100% at the beginning of the period so cannot experience large increases.

3.4 Summary

The changes to the seasonality of threshold MSDI occurrence are very similar to those for MSDI, discussed in Section 2.5. The percentage increases in the summer peak percentiles are generally much larger although this has a distinctly different meaning. Taking the 99th percentile as an example (Figure 3.1), there is currently one February day every three years on which ~60% of the TWWHA is subject to MSDI > 50, while by the end of the century this is projected to increase to ~90% of the TWWHA. The number of days per fire season that MSDI > 50 at any given location in the TWWHA is projected to triple by the end-of-century.
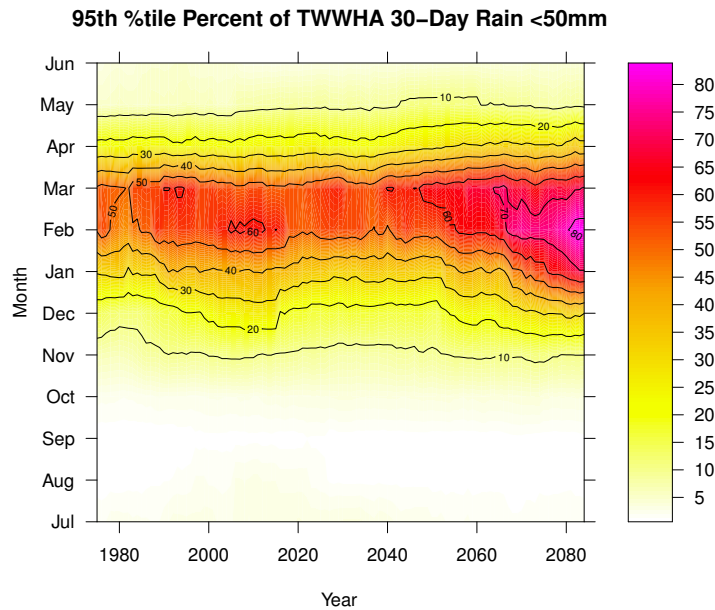
Figure 3.2: Multi-model mean projection of 95th percentile of area within TWWHA subject to 30-day antecendent rainfall less than 50 mm, calculated for each calendar month in 30-year windows stepped at 1-year intervals through the period of 1961-2100.

The changes in 30-day antecedent rainfall begin in the near future and are confined to summer and autumn. This is a tendancy towards much more widespread occurrences of these dry periods. At higher percentiles the summer peak is already close to 100% of the TWWHA so large increases in extent are not possible.The number of days per fire season on which the dry period criterion is met at any given location in the TWWHA is projected to triple by the end-of-century.

In the Adjacent Areas these indicators show a very dramatic change in conditions with mean daily extent of affected area increasing from near zero percent to around 10% and 6% for MSDI > 50 and dry periods respectively. This is driven by a trend towards much more common smaller outbreaks as well as larger extreme events.

16

4 Dry Lightning Potential Environments

4.1 Analysis Methods

The TWWHA area was examined to identify projected future dry lightning trends. Fields of "Dry Lightning Potential Environment" (DLPE) were calculated from the Climate Futures for Tasmania (CFT) model using the approach of *Rorig and Ferguson* [1999], together with the use of modest upward vertical motion (as operationally implemented in the Australian Bureau of Meteorology National Thunderstorm Forecast Guidance System, [*Deslandes et al.*, 2008]).

Grid cells conducive to the occurrence of thunderstorms were identified by the coincidence of three criteria: 850–500 hPa temperature difference in excess of 28 °C; difference between 850 hPa drybulb and dewpoint temperatures in excess of 10 °C; and upward vertical motion in excess of 10 hPa/hr.

For each day within the CFT dataset, four times were available for the calculation of the DLPE: 0600, 1200, 1800 and 2400 UT. Annual average values of the daily count of DLPE were calculated for each time, as were the corresponding 99th percentile DLPE count. Thus, for example, if 2020 has an annual average DLPE value of 3 at 1800 UT, that indicates that on average across the year, three grid cells within the TWWHA were conducive to dry lightning occurrence at 1800 UT each day.

A comprehensive series of plots of the annual and seasonal changes in DLPE are given in Appendix C. Each plot consists of a 30-year running mean of values, to reduce the influence of interannual variability, which will be a feature of the free-running models and not reflective of the trend resulting from climate change. Each of the six CFT downscaled general circulation model values of DLPE are plotted in colour, together with a MMM value in bold black. Year is plotted on the x-axis, noting that the first thirty years of the CFT time period is not available due to the requirement to compute the 30 year running mean. The count of annual average and 99th percentile values of the number of grid cells within the TWWHA which meet the criteria for DLPE are displayed on the y-axis.

4.2 DLPE Projections

To illustrate the general trend in DLPE, the time-series plot of annual mean and 99th percentile DLPE at 1200 UT are shown in Figure 4.1. This suggests a decline in the average DLPE across all models with time. Of course, average conditions do not represent the conditions under which lightning outbreaks occur although they are useful, setting the background against which such outbreaks may occur, and suggesting that the latter will be less likely to

17

occur. Again, in the 99th percentile DLPE, a gradual decline through time is evident, although with greater variability than was the case for the average.

This is consistent with the work of *Dowdy and Mills* [2012], where instability is projected to decrease with time, over the Australian region during the current century. This does not mean there will be no storms, or indeed a decline in activity levels of storms, it could be that storms may become more intense, just slightly less frequent.
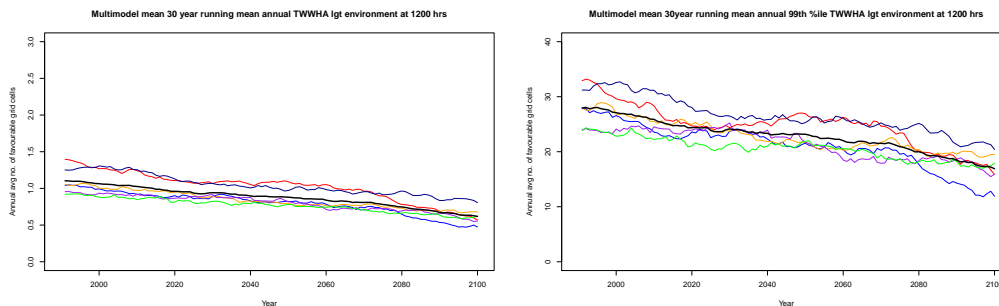
Figure 4.1: 30-year running mean of annual average (left) and 99th percentile (right) 1200 UT dry lightning potential environment over the TWWHA. Coloured lines indicate individual model values, the heavier black line shows the multi-model mean.

In general, the plots of annual DLPE reflect the changes that are projected on a seasonal basis (Appendix C). There is a decline across the seasons in the projected occurrence of suitable environments. Autumn levels of DLPE are lowest in both the average and 99th percentile values, likely a reflection of generally more stable conditions in Tasmania during that season.

Average values of DLPE are more consistent between models than are 99th percentile values. Within individual models, there is very substantial interannual and interdecadal variability in 99th percentile values, despite the plotted values being 30 year running means. It is, however, overwhelmingly the case that there is a decline in 99th percentile DLPE from the start to end of the series for each model.

While there are some diurnal variations both annually and seasonally, for no available time of day (0600, 1200, 1800 and 2400) and no season is there a projected increase in the DLPE, in either the average or 99th percentile values. The minima in the diurnal cycles of both mean and 99th percentile DLPE occur consistently at 0600 UT across all seasons except for summer. In summer the maximum in the diurnal cycles occurs at 0600 UT. This time corresponds to mid-afternoon local time which is typically when the strongest convective activity and therefore highest DLPE would be anticipated. So, it

may be that summer is the only season in which there is a sufficiently deep boundary layer to reflect diurnal surface heating at 850 hPa in CCAM.

Plotting the seasonal evolution of DLPE in the same manner as for the dryness thresholds, the seasonality in the occurence of DLPE varies significantly between lower and higher percentiles (Figure 4.2). More frequent events covering mostly very small areas of the TWWHA occur during winter and are projected to steadily decrease in areal extent throughout the CFT period. The largest, less frequent events covering 10-15% or more of the TWWHA occur during summer and decrease in extent only slightly during the CFT period. The timing of the summer peak steadily shifts to earlier in the season through the CFT period. The full set of seasonal DLPE plots are given in Figures B-6, B-7, B-8 and B-9 in Appendix B.
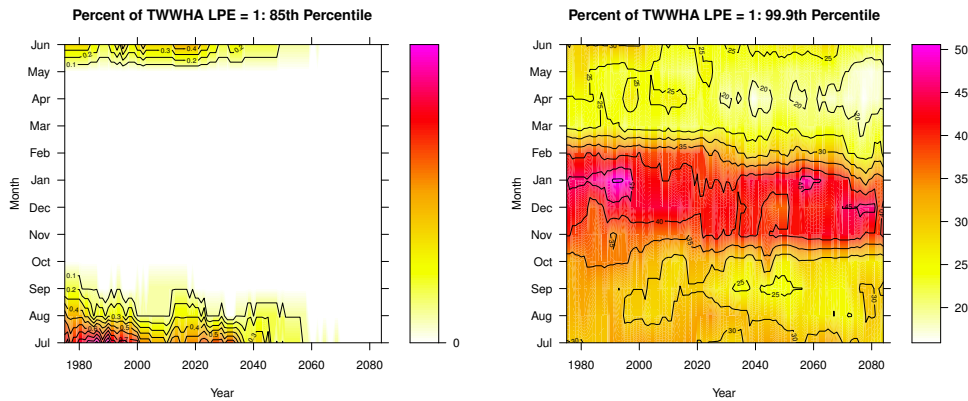
Figure 4.2: Projected multi-model mean 85th (left) and 99.9th (right) percentile 1200 UT dry lightning potential environment, calculated for each calendar month in 30-year windows stepped at 1-year intervals through the period of 1961-2100.

The time-series decrease in the mean and 99th percentile areal extent of DLPE seen in Figure 4.1 is reflected in Table A-7 in Appendix A which summarises the statistics of 1200 UT DLPE. Note that the very low values in the 85th, 90th and 99th percentiles indicate a large disparity in the distribution of DLPE event sizes. That is to say, the majority of the time the TWWHA experiences no regions of DLPE while on a small number of days it experiences wide spread DLPE. This disparity is projected to increase, but while the areal extent of the most extreme events decreases by around 10% in the near-future period it does not decrease further in the mid-century or end-of-century periods.

The characteristics are similar in the Adjacent Areas, although the mean

areal extent of DLPE is larger in the Adjacent Areas than the TWWHA. The 99th, 99.5th and 99.9th percentiles are also significantly larger for the Adjacent Areas.

Analysis of the underlying drivers of DLPE confirms that the general decline is attributable largely to the decrease in the occurence of 850–500 hPa temperature differences greater than 28 °C, particularly in autumn. The smaller temperature differences represent an increase in atmospheric stability, consistent with the projected southward migration of the subtropical ridge associated with an expansion of the tropics. Slight decreases in the 850 hPa vertical velocity are also projected during summer and autumn, while the 850 hPa dewpoint depression shows some increase during spring.

4.3   Summary

In general a steady decline is projected in the extent of DLPE outbreaks throughout the CFT period, driven largely by increasing atmospheric stability. This decrease is observed across all seasons and times of day. The steady decline is accompanied by a gradual shift of the timing of the summer DLPE peak towards earlier in the season. Given that fires in Tasmanian wilderness areas can persist for very long durations, sometimes until the end of the fire season, a tendency for ignitions earlier in the season is likely to increasingly result in the presence of fire in the landscape for most of the season. At higher percentiles the summer peak does not decrease much after near future although the duration of summer DLPE conditions becomes much shorter.

Observations indicate that in the past 15 years there has been a dramatic increase in the annual area of the TWWHA affected by lightning fire [*Styger et al.*, 2018]. This increase seems contrary to the projections of decreasing DLPE which is likely underway already. The implication is that the dramatic increases in soil and fuel dryness are more than offsetting the DLPE decrease, such that when lightning does occur fires are much more likely to be sustained. There is a need for further analysis of regional climate projections to assess changes to the frequency of coincidence of large DLPE events with high soil and fuel dryness to test this hypothesis.

5 Synoptic Patterns Over Tasmania During the 21st Century

5.1 Introduction

The CFT Future Fire Danger project highlighted changing fire danger through the twenty-first century and examined synoptic weather patterns associated with high fire danger in a number of areas of Tasmania [*Fox-Hughes et al.*, 2014, 2015]. The project demonstrated that, by the end of the current century, there was a projected increase in the number of days of elevated fire danger associated with each region's typical "bad day" synoptic pattern. However, the change in frequency of these synoptic patterns over Tasmania remained unknown. Synoptic surface pressure patterns summarise the weather conditions likely to be experienced over their domains. For fire managers in Tasmania, such patterns provide an indication of which areas might be suitable for fuel reduction burning at different times of the year, or which may require supplementation of fire suppression resources. There is a clear interest in knowing whether there will be a change in the frequency of particular synoptic patterns in the future. In general, warmer season north to north-westerly winds are associated with the worst fire danger conditions experienced in Tasmania, which includes a high degree of atmospheric instability. The northwest Tasmanian fires that occurred during the 2015-16 summer were characterised by persistent easterly and north-easterly winds that were offshore and therefore drier than usual over most of the fire grounds. The prospect of such conditions becoming more common is of considerable interest to fire and land managers tasked with the protection of the TWWHA. Knowing whether the frequency of such conditions is likely to change over coming decades will be an important consideration for fire managers, potentially affecting the size of windows of opportunity available to conduct management burns.

5.2 Analysis Methods

To gauge the likelihood of changes in the frequency of typical synoptic patterns over Tasmania, pressure gradient information was derived from the daily surface pressure fields available from the CFT high resolution models. The locations of the points sampled to derive synoptic patterns are shown as blue dots in Figure 5.1. Pressure gradients obtained from these samples were classified into compass direction, and further classified according to the strength of the pressure gradient (and, therefore of the winds over Tasmania). For example, occasions on which the difference between the top right

and bottom left points exceeded the differences between other pairs of corner points were classified as north-westerly streams. If the pressure gradient exceeded 8 hPa, the stream was classified as a strong north-westerly stream.
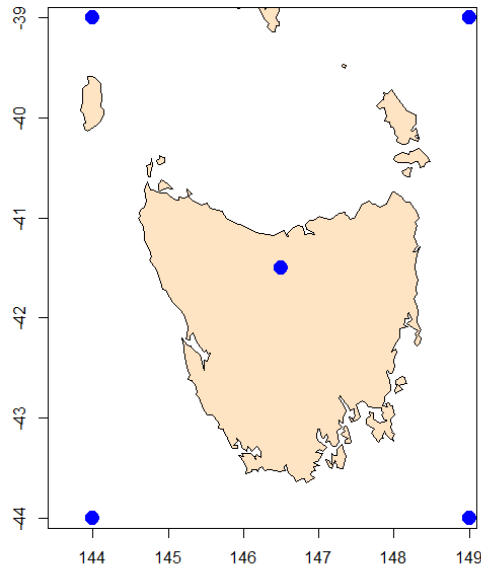
Figure 5.1: Location of pressure sample points used to derive synoptic patterns over Tasmania.

In addition, two other classifications were used. One corresponded to anticyclonic conditions, when the pressure was higher over the central pressure sample point than over surrounding points. The other corresponded to cyclonic conditions, with lower pressure over Tasmania than its surroundings. For each synoptic type, plots were generated of the change in the annual number of occurrences of that type through time, for each CFT model. A MMM of the annual count was calculated for each type, together with a 30-year running mean of the MMM annual count of occurrences of that type.

It should be noted that the typing used above could be varied slightly. One could choose a low, positive but non-zero, pressure difference across Tasmania below which the stream was classified as "Anticyclonic", for example, to reflect the fact that a synoptic pattern could reasonably be regarded as anticyclonically dominated despite there being a small pressure gradient across the island. The scheme used was chosen as being simple and clear. The criterion for a "strong" stream was used as it approximated the system used for many years in Tasmanian fire weather forecasting to identify situations

22

in which seabreezes would be excluded from forming on lee coasts, thereby increasing fire dangers experienced in those areas [*Marsh*, 1987].

5.3 Projected changes in synoptic patterns

In Figure 5.2, annual counts of each model are displayed as thin lines, the MMM of annual count is the bold red line, and the 30-year running mean of the MMM is the black dashed line. The figure shows clearly a considerable interannual variation, and variation between models, of the count of north-easterly conditions over Tasmania (ie with lower pressure to the northwest of the state and higher pressure to the southeast). There is a suggestion of a slight increase in the number of days of such north-easterly flow during the current century, but it is not a strong trend. Overall, initial analysis suggests that there are no strong trends within any of the synoptic types on an annual basis. The complete set of annual plots is displayed in Figure D-1 in Appendix D. Note that the y-axis scale varies between plots to best display the data.
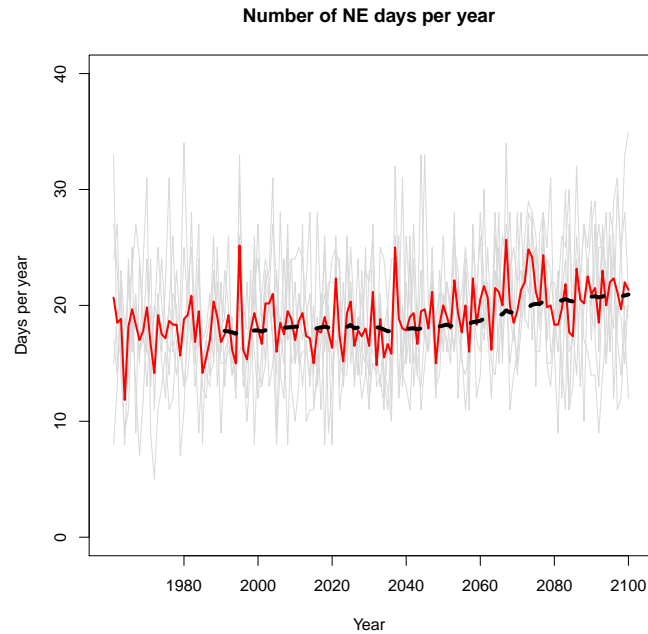

Figure 5.2: multi-model mean days per year on which north-easterly conditions occur. Annual counts of each model are displayed as thin grey lines, the multi-model mean annual count is the bold red line, and the 30-year running mean of the multi-model mean is the black dashed line.

The breakdown of synoptic type by season is displayed in Figures D-2 to D-5. Little change is projected in the MMM for winter or spring. In summer, however, and to a generally smaller extent in autumn, there is evidence of a trend through the current century for an increase in easterly quarter types, and a decrease in westerly types, including the strong NW, W and SW streams. With easterly synoptic types being more favourable for dry weather in the TWWHA than westerly, this explains at least partially the projected increases in dryness as measured by MSDI and MF.

It is quite likely (but has not been confirmed in this work) that the trends identified above are a consequence of the southward movement of the subtropical ridge during the warmer months, a characteristic change expected as a result of global warming [*Seidel et al.*, 2008] and which current observations indicate is already occurring [*Nguyen et al.*, 2013, 2015]. This would result in a greater frequency of high pressure in favourable locations, often to the east of Tasmania, with more easterly airstreams being recorded, and fewer days of westerly weather. It would also result in drier warm season conditions in western Tasmania, as identified in the previous sections.

5.4 Summary

There are no strong projected trends in the frequency with which synoptic patterns occur on an annual basis. In summer and to some extent in autumn, there is evidence of an increase in weather patterns favouring easterly winds, and a decrease in strong northwesterly to southwesterly streams. The projected increases in MSDI noted in previous sections can be attributed, at least partially, to these changes in synoptic patterns.

Appendix A: Statistics of changes to fire danger indices

Table A-1: McArthur Forest Fire Danger Index (FFDI). Statistics are multi-model mean calculated over the 20-year periods at each grid cell and averaged over the TWWHA (top panel) or Adjacent Areas (bottom panel). Quantities in parentheses are percentage change over baseline period.

TWWHA

Period	Mean	85th Perc.	90th Perc.	95th Perc.	99th Perc.	99.5th Perc.	99.9th Perc.
October–March							
1980–2000	2.64	5.13	6.68	9.72	18.13	21.83	29.80
2010–2030	2.79 (5.9)	5.47 (6.5)	7.12 (6.4)	10.31 (6.0)	19.03 (5.0)	22.66 (3.8)	30.23 (1.4)
2040–2060	3.00 (14.0)	5.86 (14.2)	7.56 (13.1)	10.84 (11.5)	20.08 (10.7)	24.35 (11.6)	33.26 (11.6)
2080–2100	3.62 (37.5)	7.22 (40.7)	9.18 (37.3)	12.78 (31.4)	22.39 (23.5)	26.74 (22.5)	36.05 (20.9)
July–June							
1980–2000	1.61	3.07	4.29	6.77	14.37	18.13	26.81
2010–2030	1.70 (5.3)	3.23 (5.3)	4.54 (6.0)	7.18 (6.1)	15.19 (5.7)	19.03 (5.0)	27.52 (2.7)
2040–2060	1.82 (12.7)	3.49 (13.8)	4.88 (13.7)	7.62 (12.6)	15.86 (10.4)	20.08 (10.8)	29.99 (11.8)
2080–2100	2.15 (33.4)	4.29 (39.9)	5.99 (39.7)	9.21 (36.1)	18.00 (25.3)	22.39 (23.5)	32.57 (21.5)

Adjacent Areas

Period	Mean	85th Perc.	90th Perc.	95th Perc.	99th Perc.	99.5th Perc.	99.9th Perc.
October–March							
1980–2000	1.88	3.80	5.16	7.83	15.32	18.69	26.30
2010–2030	2.04 (8.5)	4.17 (9.6)	5.65 (9.4)	8.60 (9.9)	16.42 (7.2)	19.80 (5.9)	26.28 (-0.0)
2040–2060	2.25 (19.8)	4.56 (20.0)	6.12 (18.5)	9.14 (16.7)	17.42 (13.7)	21.35 (14.2)	29.34 (11.6)
2080–2100	2.80 (49.2)	5.87 (54.3)	7.66 (48.4)	10.97 (40.1)	20.01 (30.6)	23.94 (28.1)	32.24 (22.6)
July–June							
1980–2000	1.10	2.02	3.06	5.22	11.96	15.33	23.27
2010–2030	1.17 (7.2)	2.15 (6.9)	3.31 (8.3)	5.69 (8.9)	12.97 (8.4)	16.42 (7.2)	23.99 (3.1)
2040–2060	1.28 (17.3)	2.42 (20.1)	3.66 (19.8)	6.15 (17.8)	13.70 (14.5)	17.42 (13.7)	26.63 (14.4)
2080–2100	1.57 (43.3)	3.12 (54.7)	4.70 (53.8)	7.68 (47.0)	15.92 (33.2)	20.01 (30.5)	29.15 (25.3)

Table A-2: Buttongrass Moorland Fire Danger Index (MFDI). Statistics are multi-model mean are calculated over the 20-year periods at each grid cell and averaged over the TWWHA (top panel) or Adjacent Areas (bottom panel). Quantities in parentheses are percentage change over baseline period.

TWWHA

Period	Mean	85th Perc.	90th Perc.	95th Perc.	99th Perc.	99.5th Perc.	99.9th Perc.
October–March							
1980–2000	3.68	6.79	8.05	10.21	15.02	16.82	20.16
2010–2030	3.68 (0.0)	6.79 (-0.1)	8.05 (-0.1)	10.15 (-0.6)	14.78 (-1.6)	16.47 (-2.1)	19.63 (-2.6)
2040–2060	3.73 (1.4)	6.87 (1.1)	8.08 (0.4)	10.15 (-0.6)	14.87 (-1.0)	16.60 (-1.4)	19.85 (-1.6)
2080–2100	3.89 (5.7)	7.15 (5.2)	8.31 (3.2)	10.25 (0.3)	14.66 (-2.4)	16.40 (-2.5)	19.54 (-3.1)
July–June							
1980–2000	3.33	6.00	7.40	9.59	14.09	15.90	19.51
2010–2030	3.36 (0.8)	6.03 (0.4)	7.42 (0.3)	9.59 (0.0)	13.98 (-0.7)	15.71 (-1.2)	19.25 (-1.3)
2040–2060	3.42 (2.8)	6.17 (2.7)	7.52 (1.6)	9.66 (0.8)	14.16 (0.5)	15.92 (0.1)	19.50 (-0.0)
2080–2100	3.56 (7.0)	6.43 (7.0)	7.75 (4.7)	9.83 (2.5)	14.27 (1.3)	16.03 (0.8)	19.58 (0.4)

Adjacent Areas

Period	Mean	85th Perc.	90th Perc.	95th Perc.	99th Perc.	99.5th Perc.	99.9th Perc.
October–March							
1980–2000	3.35	6.19	7.35	9.61	14.43	16.03	18.80
2010–2030	3.35 (-0.1)	6.21 (0.3)	7.36 (0.1)	9.53 (-0.9)	14.27 (-1.1)	15.83 (-1.3)	18.69 (-0.6)
2040–2060	3.44 (2.6)	6.35 (2.4)	7.48 (1.7)	9.68 (0.6)	14.36 (-0.5)	15.98 (-0.3)	19.02 (1.2)
2080–2100	3.56 (6.3)	6.56 (5.9)	7.62 (3.6)	9.61 (-0.0)	14.04 (-2.6)	15.63 (-2.5)	18.43 (-2.0)
July–June							
1980–2000	2.90	5.23	6.47	8.57	13.17	14.88	18.15
2010–2030	2.90 (0.2)	5.23 (-0.1)	6.46 (-0.2)	8.53 (-0.6)	13.05 (-0.8)	14.75 (-0.9)	18.02 (-0.8)
2040–2060	2.98 (2.7)	5.39 (3.0)	6.59 (1.8)	8.64 (0.7)	13.15 (-0.2)	14.85 (-0.2)	18.34 (1.0)
2080–2100	3.07 (6.0)	5.59 (6.9)	6.74 (4.2)	8.68 (1.3)	13.09 (-0.6)	14.73 (-1.0)	18.01 (-0.8)

Table A-3: Mount Soil Dryness Index (MSDI). Statistics are multi-model mean calculated over the 20-year periods at each grid cell and averaged over the TWWHA (top panel) or Adjacent Areas (bottom panel). Quantities in parentheses are percentage change over baseline period.

TWWHA

Period	Mean	85th Perc.	90th Perc.	95th Perc.	99th Perc.	99.5th Perc.	99.9th Perc.
October–March							
1980–2000	14.84	30.27	35.74	44.16	62.12	68.02	73.84
2010–2030	16.39 (10.4)	33.81 (11.7)	39.76 (11.2)	48.36 (9.5)	63.04 (1.5)	67.25 (-1.1)	72.23 (-2.2)
2040–2060	18.76 (26.4)	37.78 (24.8)	44.21 (23.7)	54.26(22.9)	73.39(18.1)	79.02(16.2)	86.81(17.6)
2080–2100	26.93 (81.5)	54.25 (79.2)	62.78 (75.7)	74.78(69.4)	95.48(53.7)	101.13(48.7)	107.70(45.8)
July–June							
1980–2000	9.69	22.14	28.22	37.53	56.12	63.15	72.69
2010–2030	10.77 (11.2)	24.68 (11.5)	31.61 (12.0)	41.71(11.2)	58.83 (4.8)	63.96 (1.3)	71.24 (-2.0)
2040–2060	12.37 (27.7)	28.12 (27.0)	35.60 (26.1)	46.53(24.0)	67.39(20.1)	74.66(18.2)	85.50(17.6)
2080–2100	17.85 (84.3)	41.78 (88.7)	51.57 (82.7)	65.60(74.8)	89.19(58.9)	96.90(53.4)	106.43(46.4)

Adjacent Areas

Period	Mean	85th Perc.	90th Perc.	95th Perc.	99th Perc.	99.5th Perc.	99.9th Perc.
October–March							
1980–2000	9.66	21.07	25.78	33.22	49.19	54.21	60.17
2010–2030	11.17 (15.5)	25.09 (19.1)	30.56 (18.6)	38.17(14.9)	51.21 (4.1)	55.40 (2.2)	60.74 (0.9)
2040–2060	13.01 (34.6)	28.05 (33.1)	33.70 (30.7)	42.95(29.3)	61.21(24.5)	67.28(24.1)	74.87(24.4)
2080–2100	19.87(105.6)	42.59(102.2)	50.23 (94.9)	61.01(83.6)	80.67(64.0)	86.40(59.4)	94.08(56.4)
July–June							
1980–2000	5.66	13.31	18.32	26.31	43.10	49.31	58.52
2010–2030	6.48 (14.4)	15.39 (15.6)	21.53 (17.5)	30.93(17.6)	46.44 (7.8)	51.40 (4.2)	59.25 (1.2)
2040–2060	7.59 (34.0)	18.04 (35.6)	24.62 (34.4)	34.48(31.1)	54.42(26.3)	61.56(24.8)	73.21(25.1)
2080–2100	11.53(103.5)	28.83(116.6)	37.92(107.0)	51.29(94.9)	73.97(71.6)	81.51(65.3)	92.12(57.4)

Table A-4: Buttongrass moorland dead-fuel Moisture Factor (MF). Statistics are multi-model mean calculated over the 20-year periods at each grid cell and averaged over the TWWHA (top panel) or Adjacent Areas (bottom panel). Quantities in parentheses are percentage change over baseline period.

TWWHA

Period	Mean	15th Perc.	10th Perc.	5th Perc.	1st Perc.	0.5th Perc.	0.1st Perc.
October–March							
1980–2000	62.26	18.19	14.48	11.38	8.61	8.05	7.26
2010–2030	61.60 (-1.1)	17.68 (-2.8)	14.07 (-2.9)	11.10 (-2.4)	8.45 (-1.9)	7.88 (-2.1)	7.15 (-1.5)
2040–2060	60.03 (-3.6)	16.77 (-7.8)	13.41 (-7.4)	10.80 (-5.1)	8.25 (-4.2)	7.68 (-4.6)	6.94 (-4.4)
2080–2100	56.99 (-8.5)	14.71 (-19.1)	11.97 (-17.4)	9.97 (-12.4)	7.87 (-8.7)	7.38 (-8.3)	6.73 (-7.3)
July–June							
1980–2000	70.03	23.36	19.20	13.94	9.48	8.61	7.51
2010–2030	69.53 (-0.7)	23.02 (-1.5)	18.83 (-2.0)	13.59 (-2.4)	9.27 (-2.3)	8.45 (-1.9)	7.37 (-1.9)
2040–2060	68.39 (-2.3)	22.20 (-5.0)	18.07 (-5.9)	13.03 (-6.5)	9.07 (-4.3)	8.25 (-4.2)	7.16 (-4.6)
2080–2100	66.63 (-4.9)	20.56 (-12.0)	16.46 (-14.3)	11.84 (-15.0)	8.56 (-9.7)	7.87 (-8.6)	6.93 (-7.8)

Adjacent Areas

Period	Mean	15th Perc.	10th Perc.	5th Perc.	1st Perc.	0.5th Perc.	0.1st Perc.
October–March							
1980–2000	62.40	17.55	13.84	11.15	8.53	7.95	7.15
2010–2030	61.95 (-0.7)	17.13 (-2.4)	13.49 (-2.5)	10.87 (-2.5)	8.35 (-2.1)	7.80 (-1.9)	7.08 (-0.9)
2040–2060	60.05 (-3.8)	15.91 (-9.3)	12.80 (-7.6)	10.52 (-5.7)	8.10 (-5.0)	7.56 (-4.9)	6.83 (-4.4)
2080–2100	57.33 (-8.1)	14.07 (-19.8)	11.65 (-15.9)	9.80 (-12.1)	7.75 (-9.1)	7.28 (-8.4)	6.60 (-7.6)
July–June							
1980–2000	70.65	23.31	19.02	13.53	9.39	8.53	7.40
2010–2030	70.33 (-0.5)	23.11 (-0.9)	18.76 (-1.4)	13.24 (-2.2)	9.15 (-2.5)	8.35 (-2.1)	7.29 (-1.5)
2040–2060	69.08 (-2.2)	22.15 (-5.0)	17.74 (-6.7)	12.61 (-6.8)	8.89 (-5.3)	8.10 (-5.0)	7.05 (-4.8)
2080–2100	67.62 (-4.3)	20.70 (-11.2)	16.19 (-14.9)	11.57 (-14.5)	8.41 (-10.4)	7.75 (-9.1)	6.82 (-7.8)

Table A-5: Occurence of Mount Soil Dryness Index (MSDI) greater than 50. Count is the multi-model mean number of days per fire season (Oct-Mar) or per full year (Jul-Jun) on which MSDI exceeded 50, averaged over the TWWHA (top panel) or Adjacent Areas (bottom panel). Mean and percentile statistics are for the multi-model mean areal extent as a percentage of the TWWHA where daily MSDI exceeded 50. Quantities in parentheses are percentage change over baseline period.

TWWHA

Period	Count	Mean	85th Perc.	90th Perc.	95th Perc.	99th Perc.	99.5th Perc.	99.9th Perc.
Oct–Mar								
1980–2000	10.26	5.22	11.27	15.06	22.44	51.80	60.61	70.93
2010–2030	11.87 (15.7)	6.04 (15.7)	13.35 (18.5)	17.90 (18.9)	27.08 (20.7)	49.24 (-4.9)	57.10 (-5.8)	65.25(-8.0)
2040–2060	16.18 (57.8)	8.23 (57.8)	17.80 (58.0)	24.43 (62.3)	37.41 (66.7)	66.48 (28.3)	75.47 (24.5)	85.23(20.2)
2080–2100	32.57(217.6)	16.57(217.6)	39.30 (248.7)	53.50 (255.3)	71.78 (219.8)	89.20 (72.2)	90.81 (49.8)	91.86(29.5)
Jul–Jun								
1980–2000	13.44	3.41	7.20	10.32	16.48	37.50	52.08	68.47
2010–2030	15.80 (17.6)	4.01 (17.6)	8.81 (22.4)	12.31 (19.3)	19.89 (20.7)	40.06 (6.8)	49.34 (-5.3)	62.50(-8.7)
2040–2060	21.26 (58.2)	5.39 (58.2)	11.08 (53.9)	16.29 (57.8)	26.61 (61.5)	55.78 (48.7)	66.86 (28.4)	82.58(20.6)
2080–2100	42.16(213.7)	10.70(213.7)	23.86 (231.6)	33.90 (228.4)	54.92 (233.3)	85.13(127.0)	89.20 (71.3)	91.57(33.7)

Adj. Areas

Period	Count	Mean	85th Perc.	90th Perc.	95th Perc.	99th Perc.	99.5th Perc.	99.9th Perc.
Oct–Mar								
1980–2000	2.64	1.33	1.06	2.13	5.32	34.04	46.81	64.18
2010–2030	3.64 (38.0)	1.83 (38.0)	2.13 (100.0)	4.61 (116.7)	10.99 (106.7)	35.46 (4.2)	46.81 (0.0)	60.28(-6.1)
2040–2060	6.49(146.0)	3.26(146.0)	3.90 (266.7)	7.80 (266.7)	21.28 (300.0)	58.87 (72.9)	67.38 (43.9)	80.85(26.0)
2080–2100	19.45(636.8)	9.78(636.8)	22.70(2033.3)	36.52(1616.7)	62.06(1066.7)	86.88(155.2)	89.01 (90.2)	90.78(41.4)
Jul–Jun								
1980–2000	2.82	0.71	0.00	0.71	2.13	19.50	34.04	57.09
2010–2030	3.86 (36.6)	0.97 (36.6)	0.00 (0.0)	2.13 (200.0)	4.61 (116.7)	23.40 (20.0)	35.46 (4.2)	56.74(-0.6)
2040–2060	7.09(151.0)	1.78(151.0)	1.06 (n/a)	2.48 (250.0)	8.51 (300.0)	43.26(121.8)	58.87 (72.9)	77.66(36.0)
2080–2100	21.18(650.2)	5.31(650.2)	6.38 (n/a)	16.31(2200.0)	38.30(1700.0)	81.91(320.0)	86.88(155.2)	90.43(58.4)

Table A-6: Occurence of 30-day dry periods (less than 50mm rain). Count is the multi-model mean number of days per fire season (Oct-Mar) or per full year (Jul-Jun) for which the 30-day antecedent rainfall was less than 50 mm, averaged over the TWWHA (top panel) or Adjacent Areas (bottom panel). Mean and percentile statistics are for the multi-model mean areal extent as a percentage of the TWWHA where the 30-day antecedent rainfall was less than 50 mm. Quantities in parentheses are percentage change over baseline period.

TWWHA

Period	Count	Mean	85th Perc.	90th Perc.	95th Perc.	99th Perc.	99.5th Perc.	99.9th Perc.
Oct–Mar								
1980–2000	9.31	5.12	8.33	13.54	27.37	69.60	85.32	96.40
2010–2030	10.04 (7.8)	5.52 (7.8)	9.56 (14.8)	15.44 (14.0)	29.92 (9.3)	71.78 (3.1)	85.61 (0.3)	95.45(-1.0)
2040–2060	11.36 (22.0)	6.24 (22.0)	11.46 (37.5)	18.84 (39.2)	33.24 (21.5)	76.70 (10.2)	90.62 (6.2)	99.62 (3.3)
2080–2100	17.81 (91.3)	9.78 (91.3)	19.98(139.8)	31.82(135.0)	57.20(109.0)	96.78 (39.0)	98.96(16.0)	100.00 (3.7)
Jul–Jun								
1980–2000	11.83	3.24	4.45	7.77	16.95	54.64	73.30	95.64
2010–2030	12.82 (8.4)	3.51 (8.4)	5.02 (12.8)	9.19 (18.3)	19.03 (12.3)	57.58 (5.4)	72.92 (-0.5)	93.37(-2.4)
2040–2060	14.32 (21.1)	3.92 (21.1)	5.97 (34.0)	10.32 (32.9)	22.54 (33.0)	60.98 (11.6)	77.37 (5.6)	98.20 (2.7)
2080–2100	21.15 (78.8)	5.79 (78.8)	8.71 (95.7)	16.29(109.8)	35.32(108.4)	87.69 (60.5)	96.78(32.0)	99.91 (4.5)

Adj. Areas

Period	Count	Mean	85th Perc.	90th Perc.	95th Perc.	99th Perc.	99.5th Perc.	99.9th Perc.
Oct–Mar								
1980–2000	3.94	2.07	0.00	1.42	9.22	57.80	77.66	92.91
2010–2030	4.85 (23.1)	2.55 (23.1)	0.35 (n/a)	2.48 (75.0)	14.18 (53.8)	65.96 (14.1)	80.14 (3.2)	93.26 (0.4)
2040–2060	5.60 (42.1)	2.95 (42.1)	1.42 (n/a)	4.96(250.0)	18.09 (96.2)	70.92 (22.7)	88.30(13.7)	95.39 (2.7)
2080–2100	10.80(173.7)	5.68(173.7)	5.32 (n/a)	15.25(975.0)	44.33(380.8)	91.49 (58.3)	95.04(22.4)	95.74 (3.1)
Jul–Jun								
1980–2000	4.33	1.14	0.00	0.00	2.13	39.01	60.64	91.13
2010–2030	5.30 (22.4)	1.39 (22.4)	0.00 (0.0)	0.00 (0.0)	3.19 (50.0)	45.74 (17.3)	67.73(11.7)	91.13 (0.0)
2040–2060	6.10 (41.0)	1.60 (41.0)	0.00 (0.0)	0.71 (n/a)	6.03(183.3)	46.81 (20.0)	71.63(18.1)	94.68 (3.9)
2080–2100	11.38(162.9)	2.98(162.9)	0.00 (0.0)	2.48 (n/a)	16.67(683.3)	82.62(111.8)	91.84(51.5)	95.74 (5.1)

Table A-7: Occurence of lightning potential environment for model time 1200 UT. Count is the multi-model mean number of days per fire season (Oct-Mar) or per full year (Jul-Jun) for which lightning potential environment was favourable, averaged over the TWWHA (top panel) or Adjacent Areas (bottom panel). Mean and percentile statistics are for the multi-model mean areal extent as a percentage of the TWWHA where lightning potential environment is favourable. Quantities in parentheses are percentage change over baseline period.

TWWHA

Period	Count	Mean	85th Perc.	90th Perc.	95th Perc.	99th Perc.	99.5th Perc.	99.9th Perc.
Oct–Mar								
1980–2000	1.02	0.57	0.00	0.00	1.61	18.75	26.14	41.57
2010–2030	0.89 (-13.2)	0.49 (-13.2)	0.00 (0.0)	0.00 (0.0)	1.23 (-23.5)	15.81 (-15.7)	23.67 (-9.4)	37.50 (-9.8)
2040–2060	0.84 (-18.0)	0.46 (-18.0)	0.00 (0.0)	0.00 (0.0)	0.85 (-47.1)	16.29 (-13.1)	24.53 (-6.2)	38.35 (-7.7)
2080–2100	0.66 (-35.2)	0.37 (-35.2)	0.00 (0.0)	0.00 (0.0)	0.28 (-82.4)	12.78 (-31.8)	22.16 (-15.2)	37.88 (-8.9)
Jul–Jun								
1980–2000	2.15	0.59	0.00	0.28	2.46	16.29	24.15	39.30
2010–2030	1.88 (-12.6)	0.52 (-12.6)	0.00 (0.0)	0.19 (-33.3)	2.08 (-15.4)	14.58 (-10.5)	21.50 (-11.0)	35.61 (-9.4)
2040–2060	1.71 (-20.6)	0.47 (-20.6)	0.00 (0.0)	0.00 (-100.0)	1.70 (-30.8)	13.64 (-16.3)	21.69 (-10.2)	36.65 (-6.7)
2080–2100	1.21 (-43.8)	0.33 (-43.8)	0.00 (0.0)	0.00 (-100.0)	0.47 (-80.8)	9.56 (-41.3)	17.71 (-26.7)	35.13 (-10.6)

Adj. Areas

Period	Count	Mean	85th Perc.	90th Perc.	95th Perc.	99th Perc.	99.5th Perc.	99.9th Perc.
Oct–Mar								
1980–2000	1.73	0.95	0.00	0.00	1.06	32.27	42.91	66.67
2010–2030	1.56 (-9.6)	0.86 (-9.6)	0.00 (0.0)	0.00 (0.0)	0.71 (-33.3)	29.08 (-9.9)	40.78 (-5.0)	64.89 (-2.7)
2040–2060	1.48 (-14.5)	0.81 (-14.5)	0.00 (0.0)	0.00 (0.0)	0.35 (-66.7)	29.43 (-8.8)	40.78 (-5.0)	61.35 (-8.0)
2080–2100	1.25 (-27.7)	0.69 (-27.7)	0.00 (0.0)	0.00 (0.0)	0.00 (-100.0)	26.24 (-18.7)	38.30 (-10.7)	62.06 (-6.9)
Jul–Jun								
1980–2000	2.57	0.70	0.00	0.00	0.71	24.47	36.52	59.57
2010–2030	2.31 (-10.2)	0.63 (-10.2)	0.00 (0.0)	0.00 (0.0)	0.00 (-100.0)	22.70 (-7.2)	34.40 (-5.8)	59.22 (-0.6)
2040–2060	2.08 (-19.1)	0.57 (-19.1)	0.00 (0.0)	0.00 (0.0)	0.00 (-100.0)	20.57 (-15.9)	33.69 (-7.8)	56.38 (-5.4)
2080–2100	1.66 (-35.5)	0.45 (-35.5)	0.00 (0.0)	0.00 (0.0)	0.00 (-100.0)	17.38 (-29.0)	30.85 (-15.5)	55.32 (-7.1)

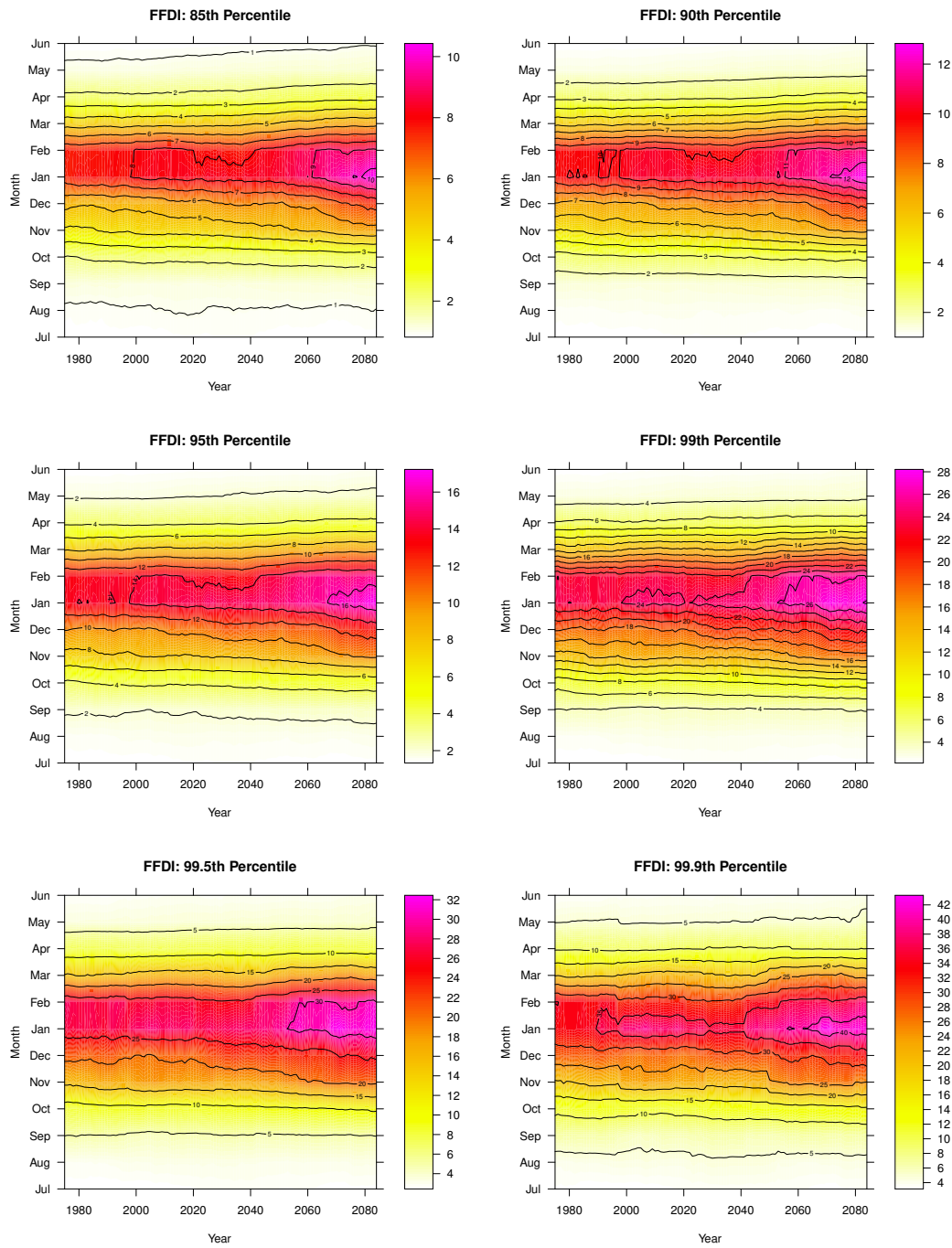# Appendix B: Seasonality of changes to fire danger indices

Figure B-1: Projected multi-model mean 85th, 90th, 95th, 99th, 99.5th and 99.9th percentile McArthur Forest Fire Danger Index averaged over the TWWHA as a function of month-of-year and year-of-period. Statistics calculated over 30-year windows.
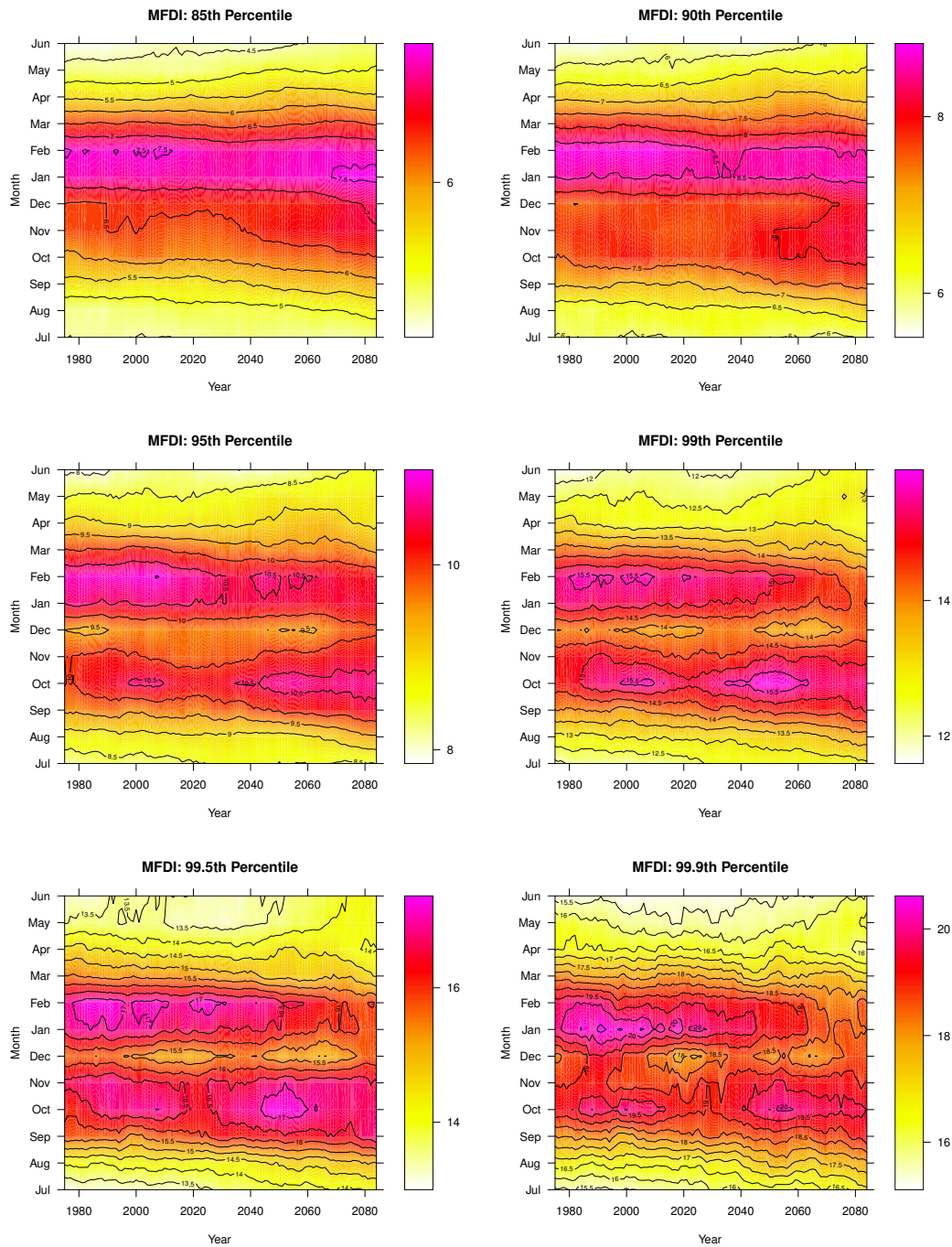
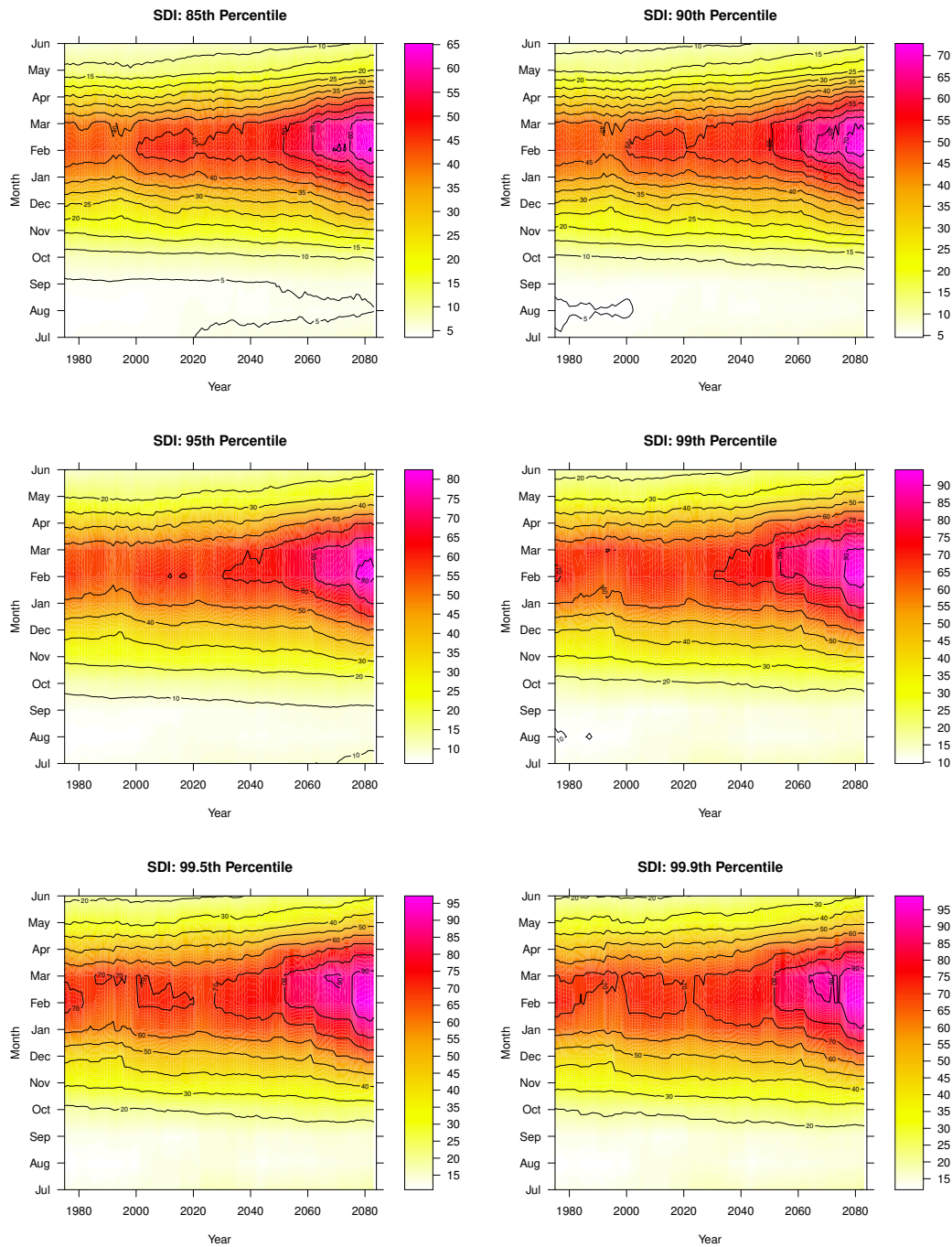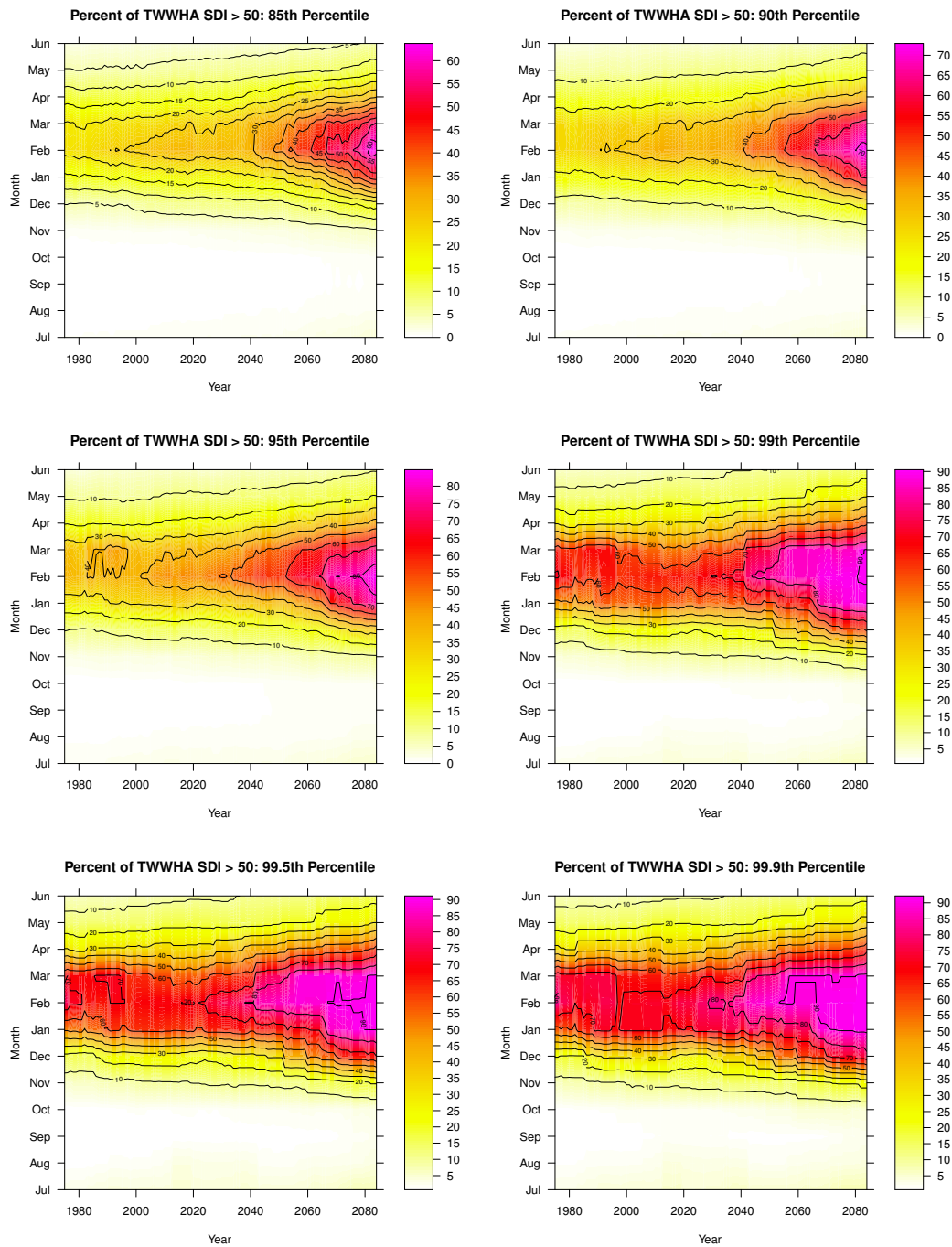Figure B-2: Projected multi-model mean 85th, 90th, 95th, 99th, 99.5th and 99.9th percentile Buttongrass Moorland Fire Danger Index averaged over the TWWHA as a function of month-of-year and year-of-period. Statistics calculated over 30-year windows.

Figure B-3: Projected multi-model mean 85th, 90th, 95th, 99th, 99.5th and 99.9th percentile Mount Soil Dryness Index averaged over the TWWHA as a function of month-of-year and year-of-period. Statistics calculated over 30-year windows.
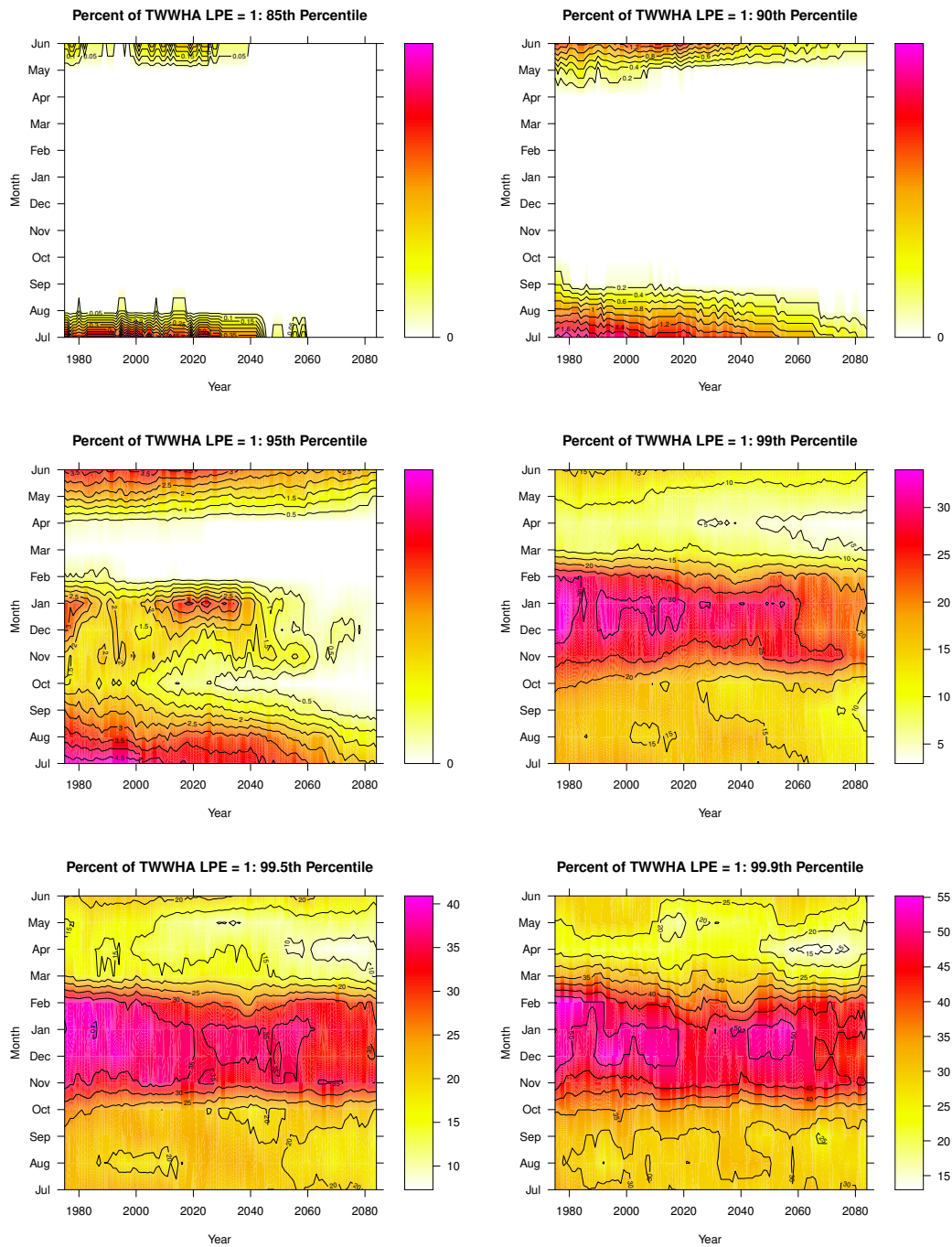
Figure B-4: Projected multi-model mean 85th, 90th, 95th, 99th, 99.5th and 99.9th percentile areal extent as a percentage of the TWWHA where Mount Soil Dryness Index is greater than 50, as a function of month-of-year and year-of-period.
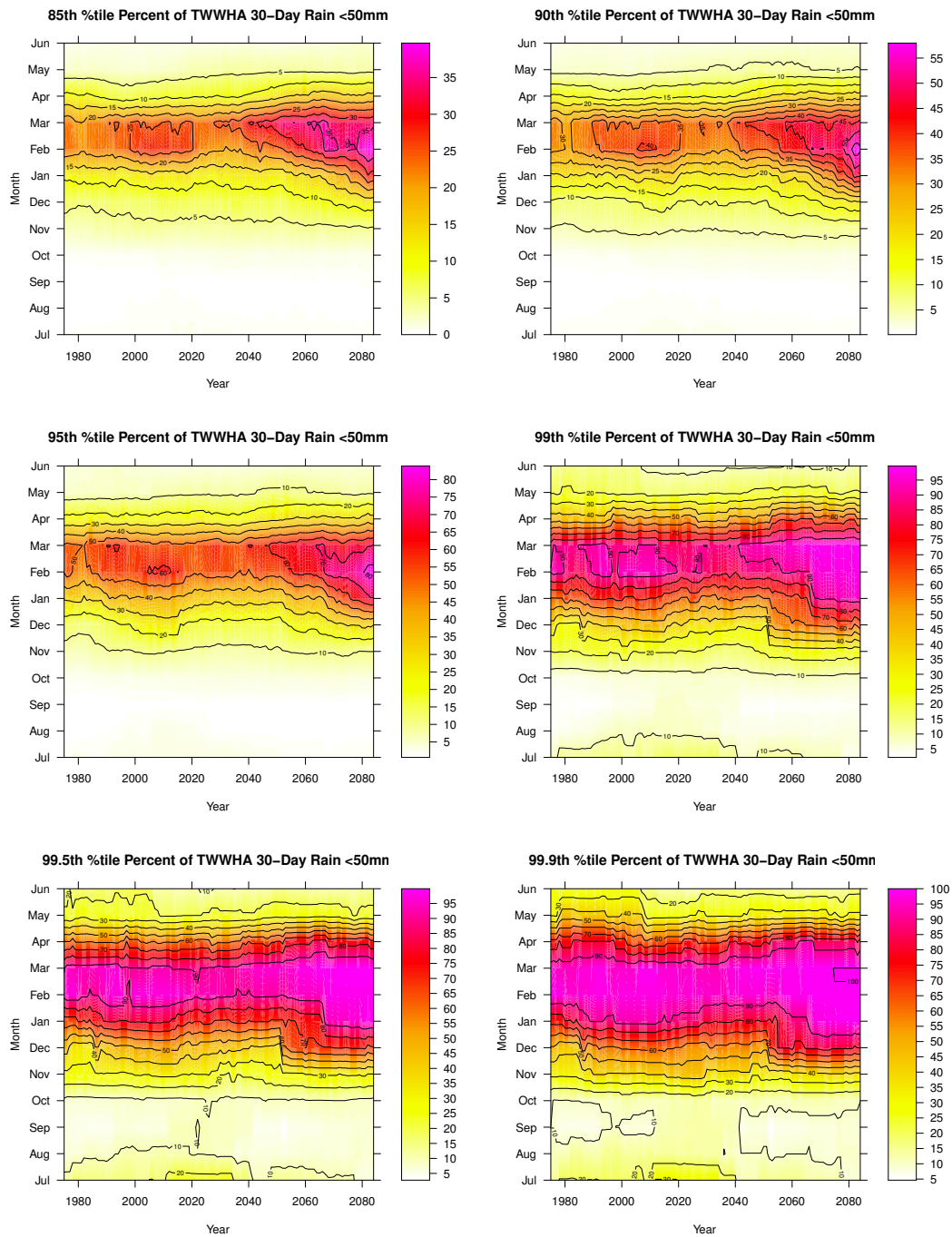
Figure B-5: Projected multi-model mean 85th, 90th, 95th, 99th, 99.5th and 99.9th percentile areal extent as a percentage of the TWWHA where 30-day antecedent rainfall is less than 50 mm, as a function of month-of-year and year-of-period.
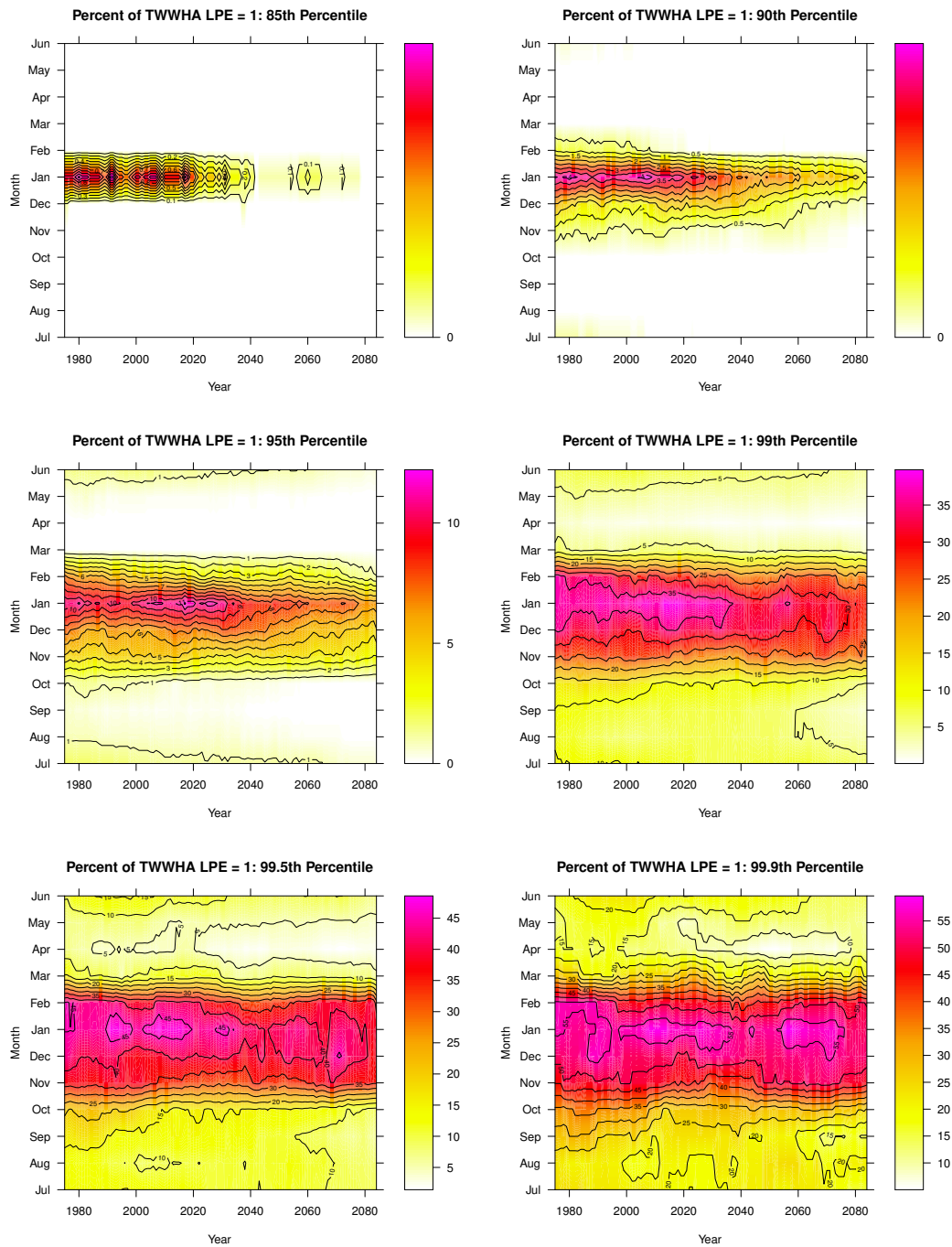
Figure B-6: Projected multi-model mean 85th, 90th, 95th, 99th, 99.5th and 99.9th percentile areal extent as a percentage of the TWWHA where dry lightning potential environment is favourable at 0600 UT, as a function of month-of-year and year-of-period.
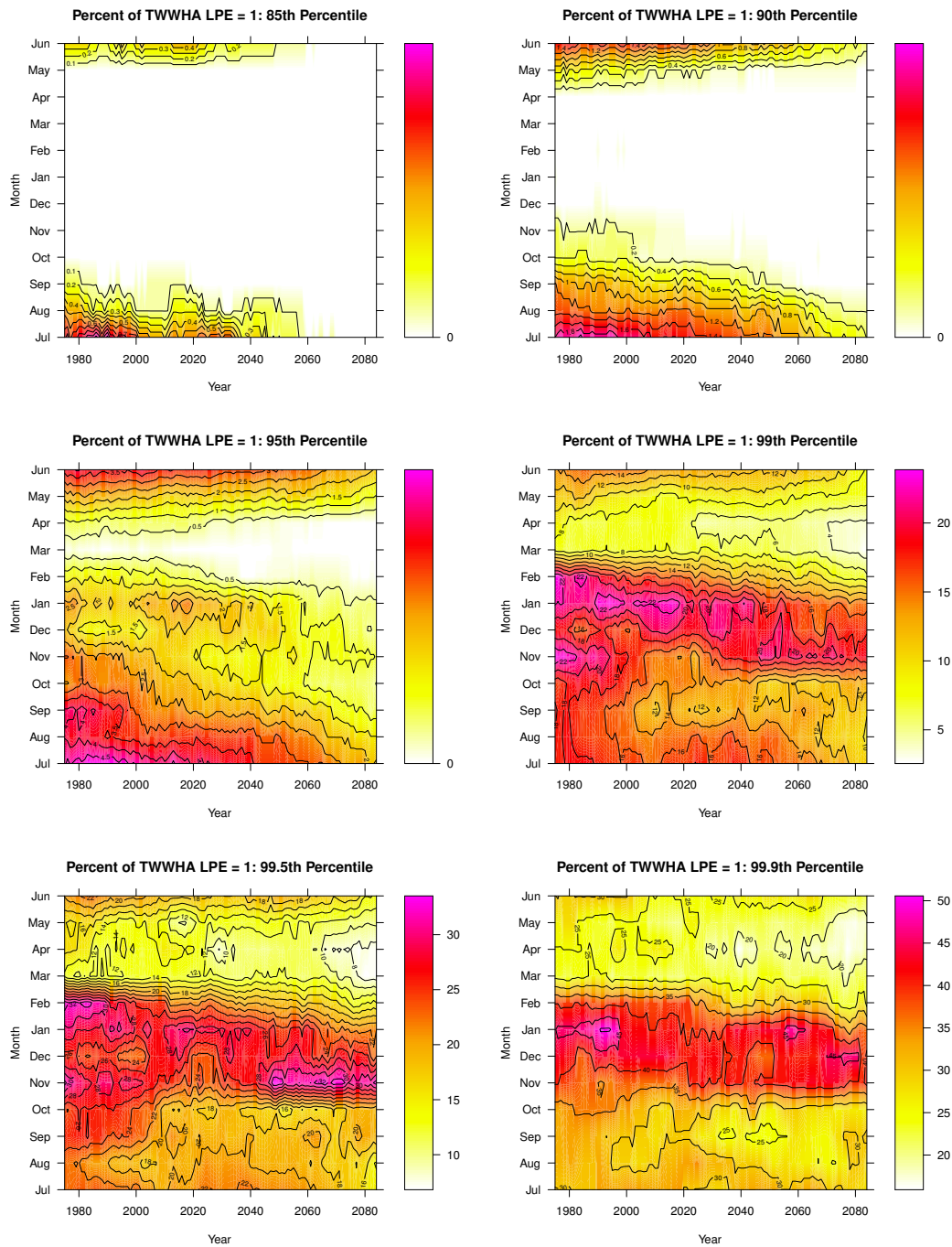
Figure B-7: Projected multi-model mean 85th, 90th, 95th, 99th, 99.5th and 99.9th percentile areal extent as a percentage of the TWWHA where dry lightning potential environment is favourable at 1200 UT, as a function of month-of-year and year-of-period.
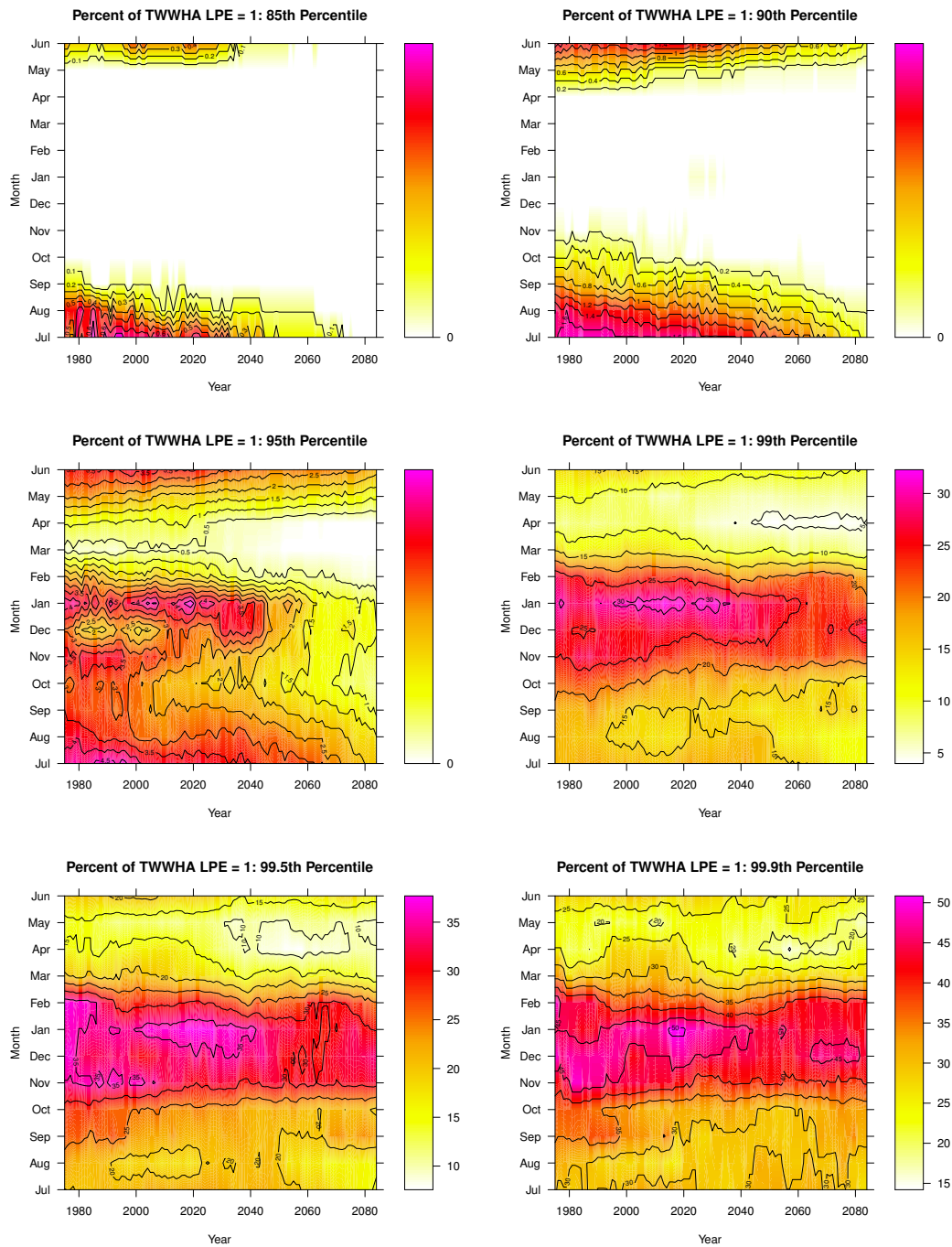
Figure B-8: Projected multi-model mean 85th, 90th, 95th, 99th, 99.5th and 99.9th percentile areal extent as a percentage of the TWWHA where dry lightning potential environment is favourable at 1800 UT, as a function of month-of-year and year-of-period.

Figure B-9: Projected multi-model mean 85th, 90th, 95th, 99th, 99.5th and 99.9th percentile areal extent as a percentage of the TWWHA where dry lightning potential environment is favourable at 0000 UT, as a function of month-of-year and year-of-period.

Appendix C: Dry Lightning Potential Environment projections
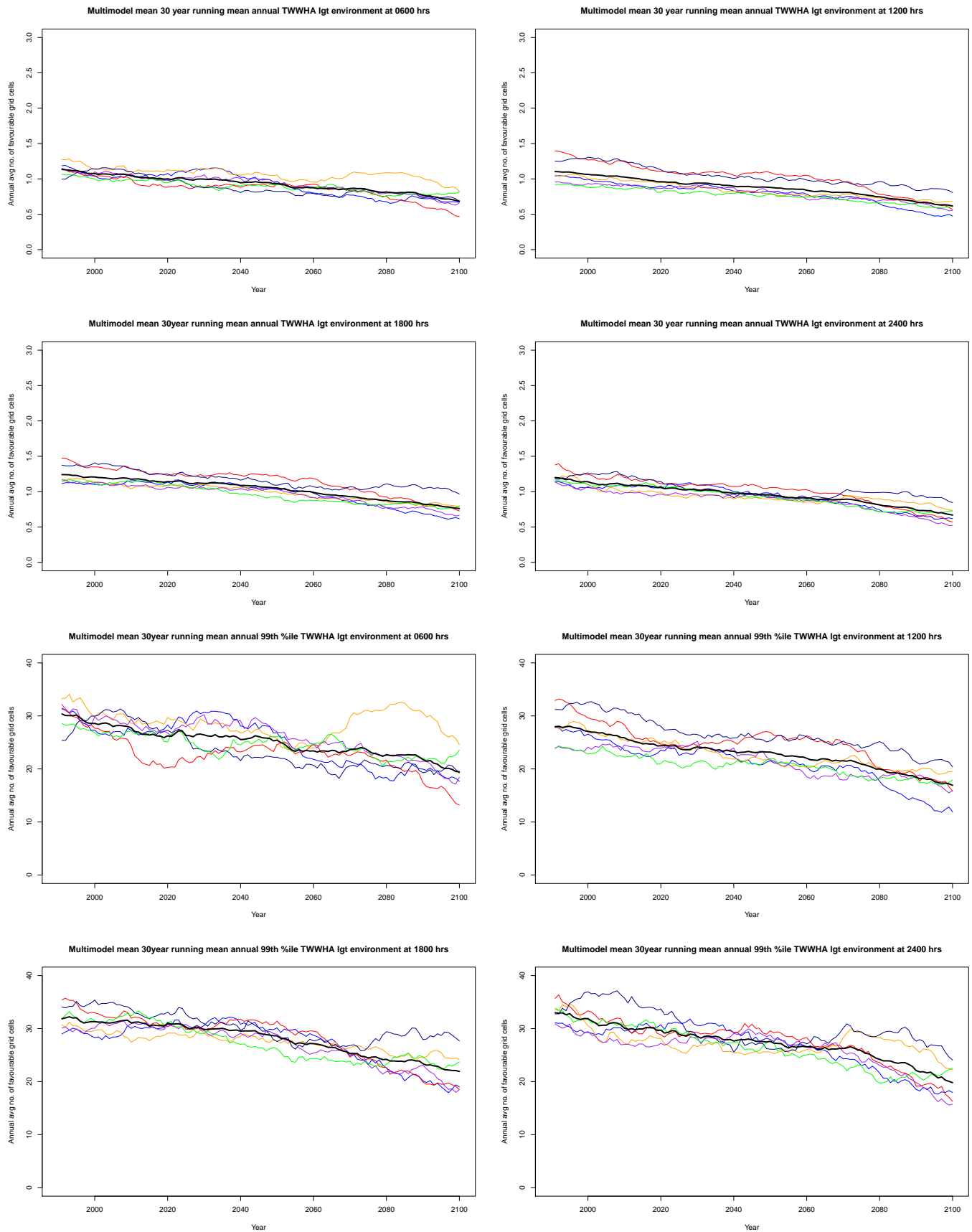
Figure C-1: Annual Dry Lightning Potential Environment mean and 99th percentile. Coloured lines are individual models, black line is the multi-model mean. Individual models and multi-model mean have been smoothed with 30-year running mean.
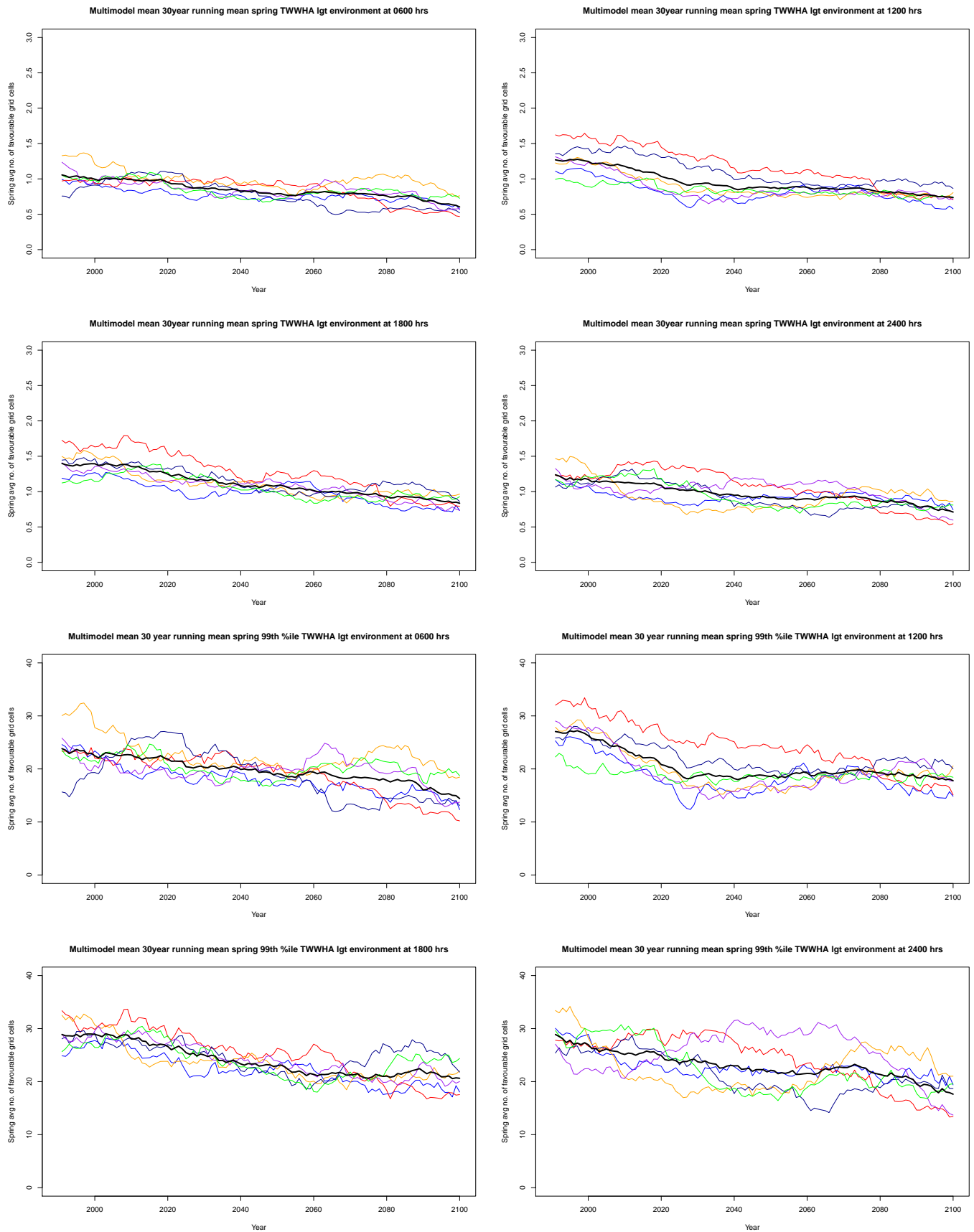
Figure C-2: Spring Dry Lightning Potential Environment mean and 99th percentile, as for Figure C-1
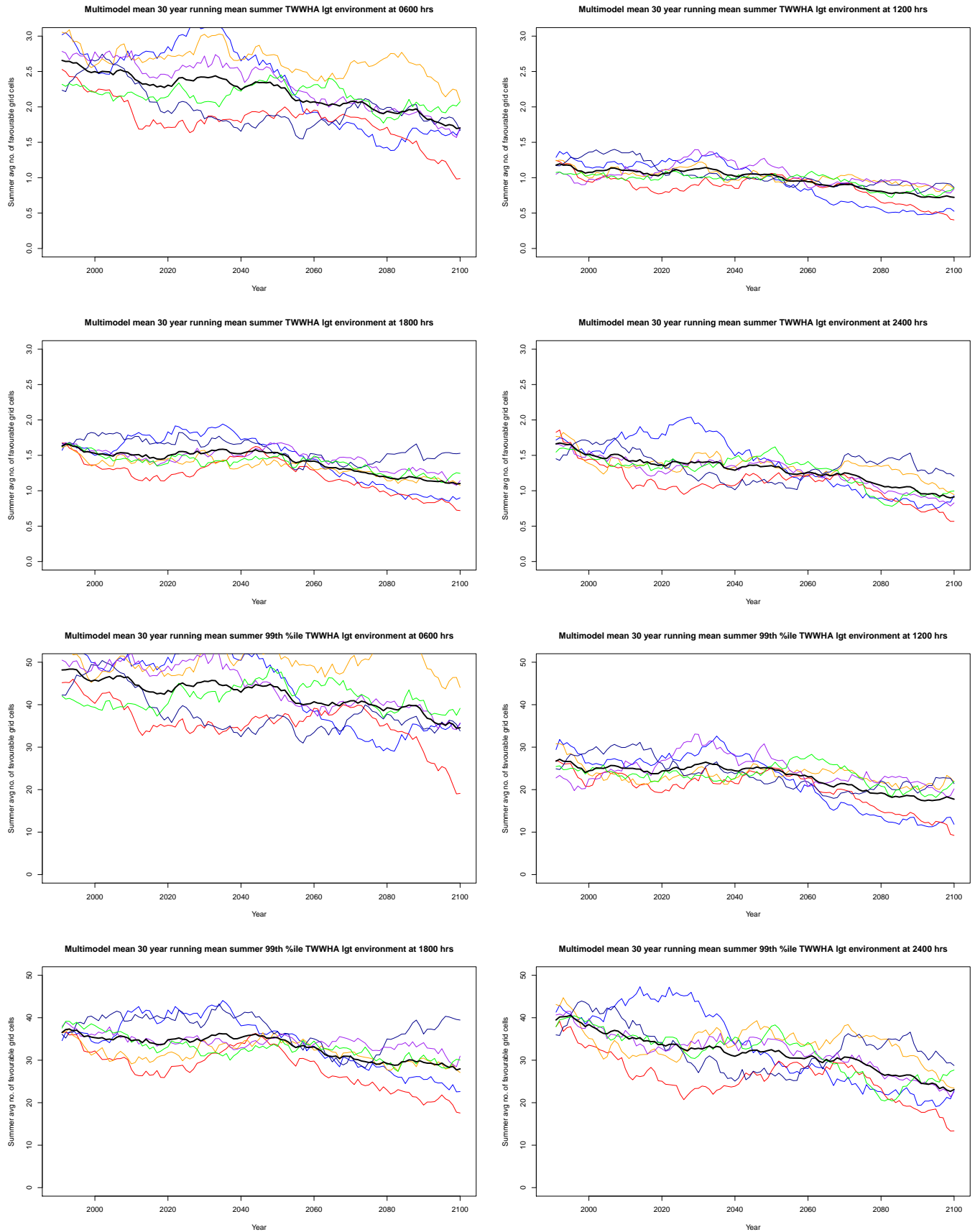
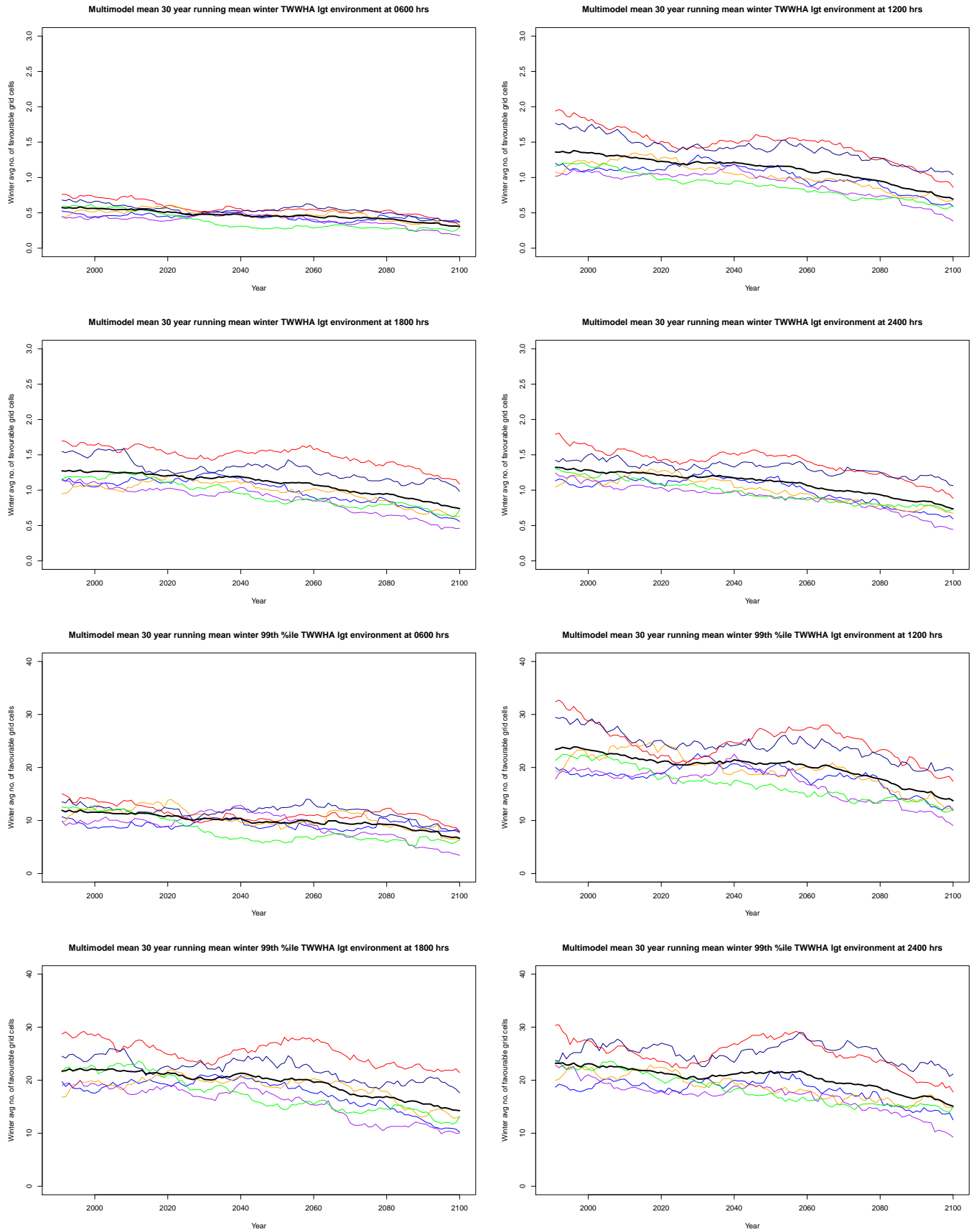Figure C-3: Summer Dry Lightning Potential Environment mean and 99th percentile, as for Figure C-1
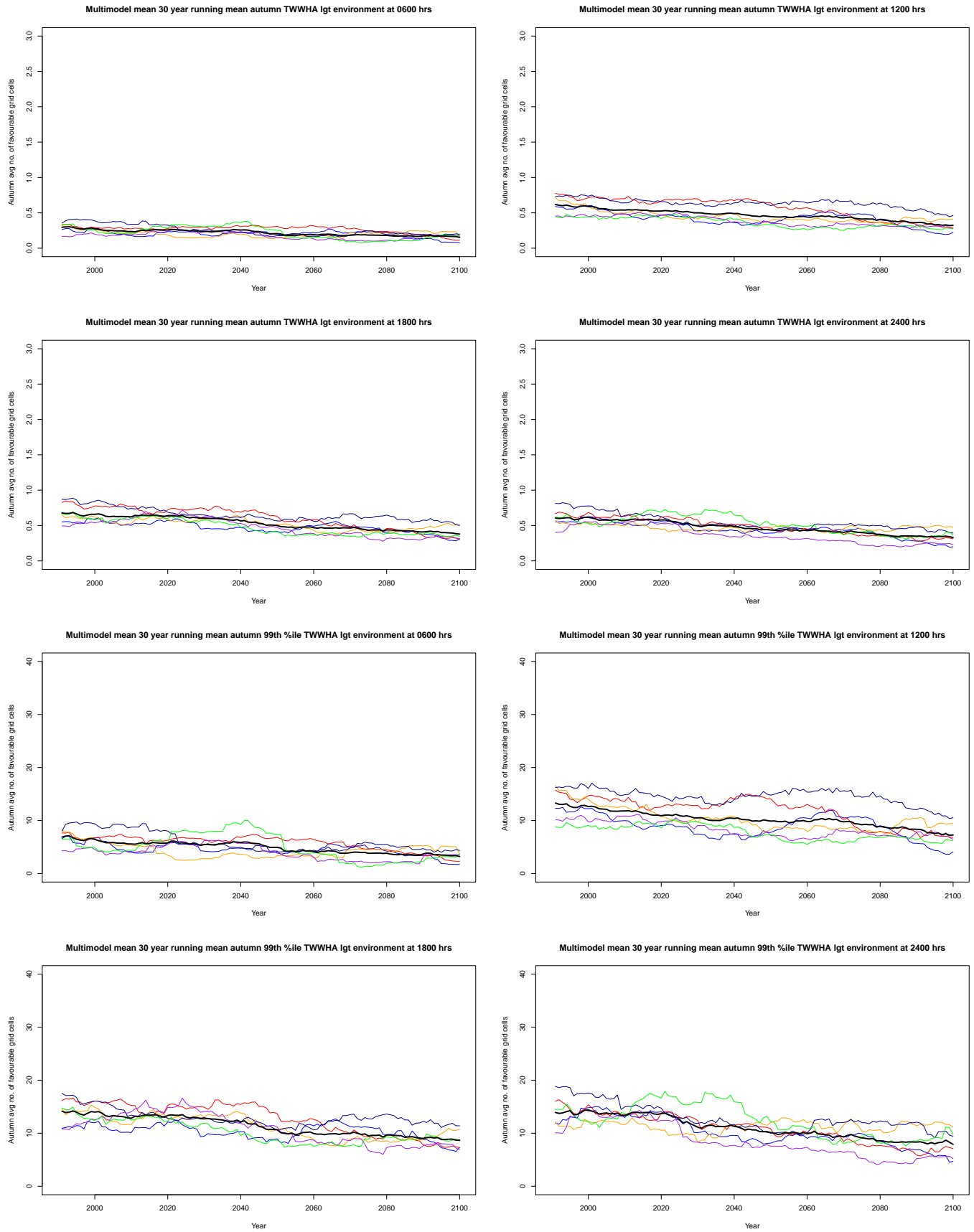
Figure C-4: Autumn Dry Lightning Potential Environment mean and 99th percentile, as for Figure C-1

Figure C-5: Winter Dry Lightning Potential Environment mean and 99th percentile, as for Figure C-1
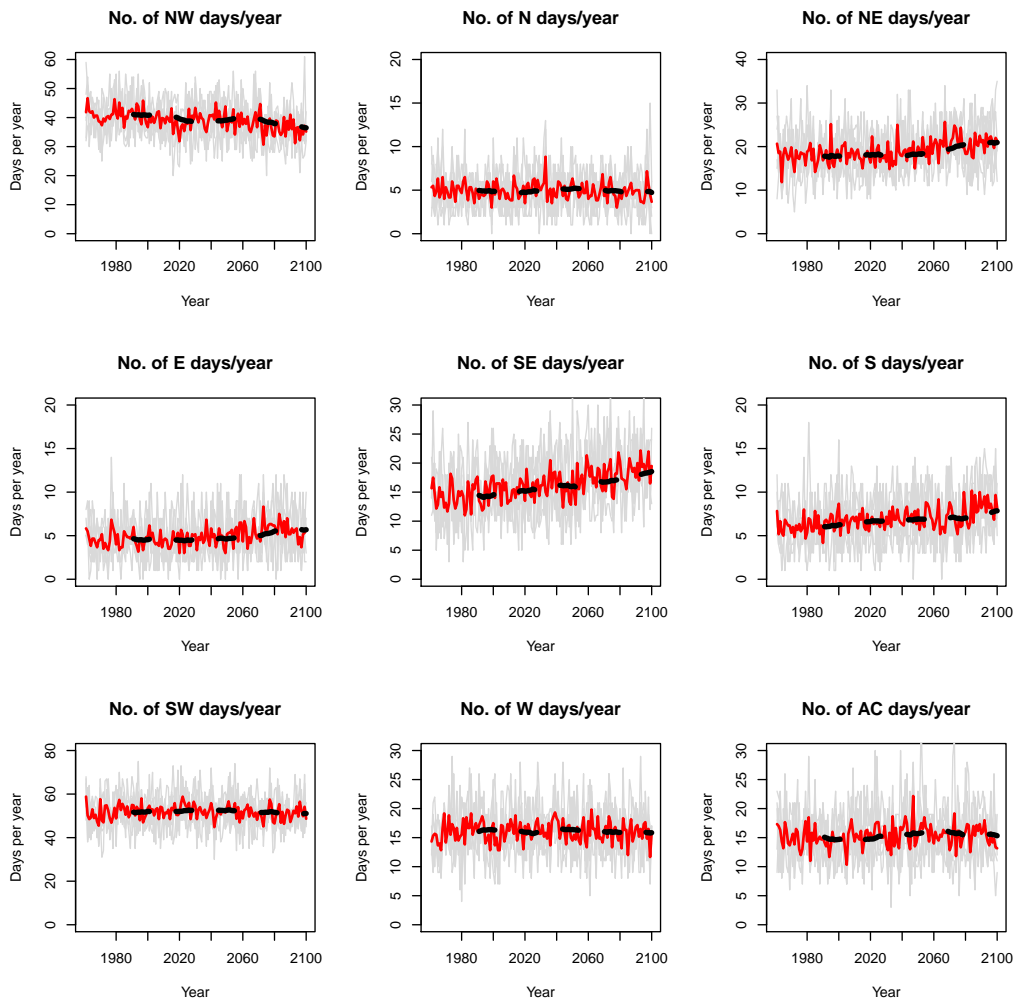
Appendix D: Projected synoptic pattern climatology

Figure D-1: Changes in annual frequencies of synoptic patterns. Annual counts of each model are displayed as thin grey lines, the multi-model mean of the annual count is the bold red line, and the 30 year running mean of the multi-model mean is the black dashed line. (AC = Anticyclonic, CYC= Cyclonic, the "str" prefix indicates strong winds).
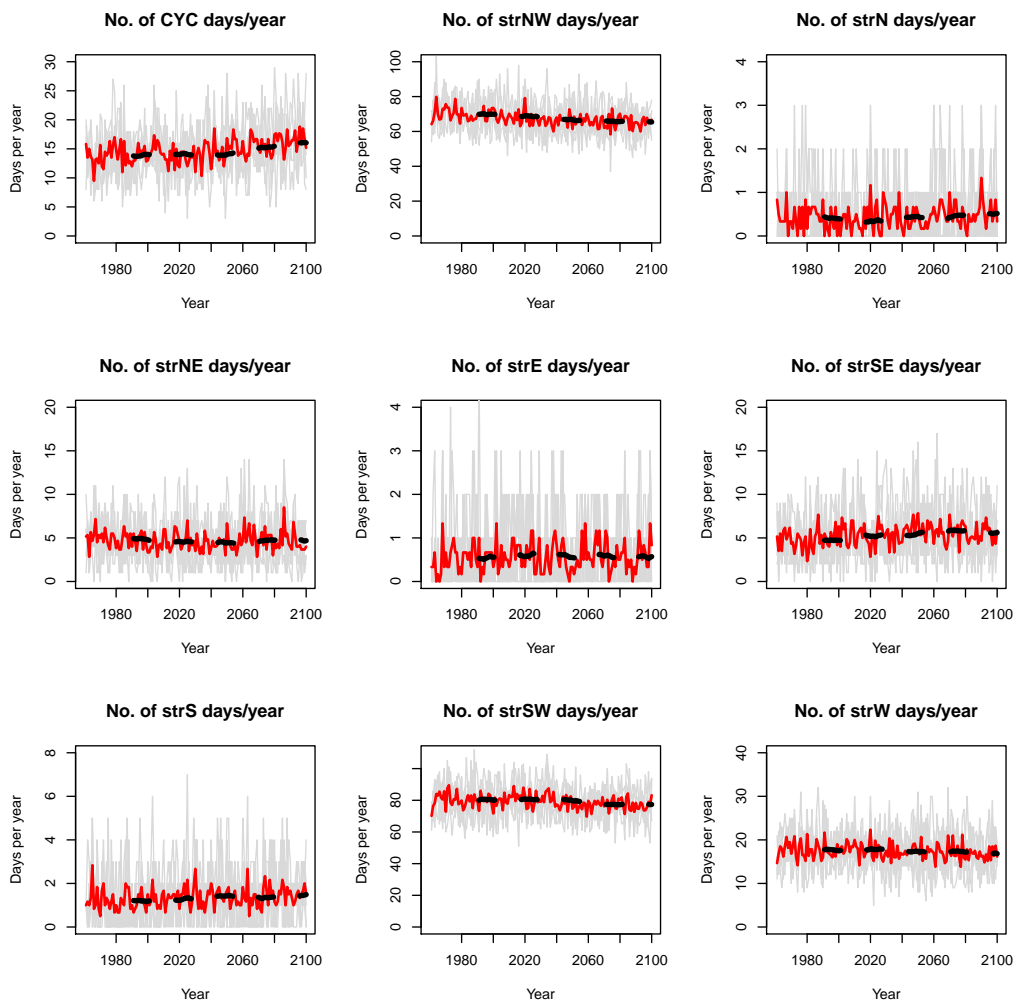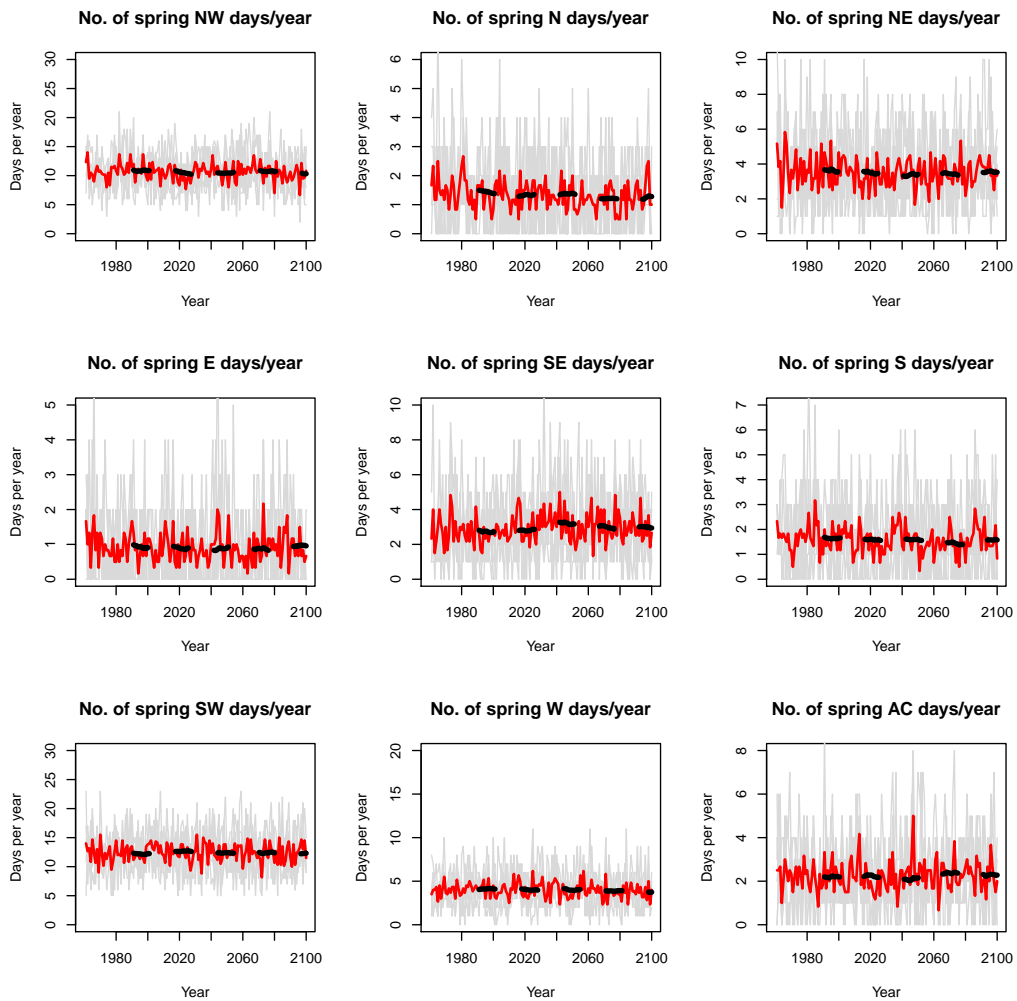
Figure D-1: Cont.

51

Figure D-2: Changes in spring frequencies of synoptic patterns. Annual counts of each model are displayed as thin grey lines, the multi-model mean of the annual count is the bold red line, and the 30 year running mean of the multi-model mean is the black dashed line. (AC = Anticyclonic, CYC= Cyclonic, the "str" prefix indicates strong winds). (Cont. next page)
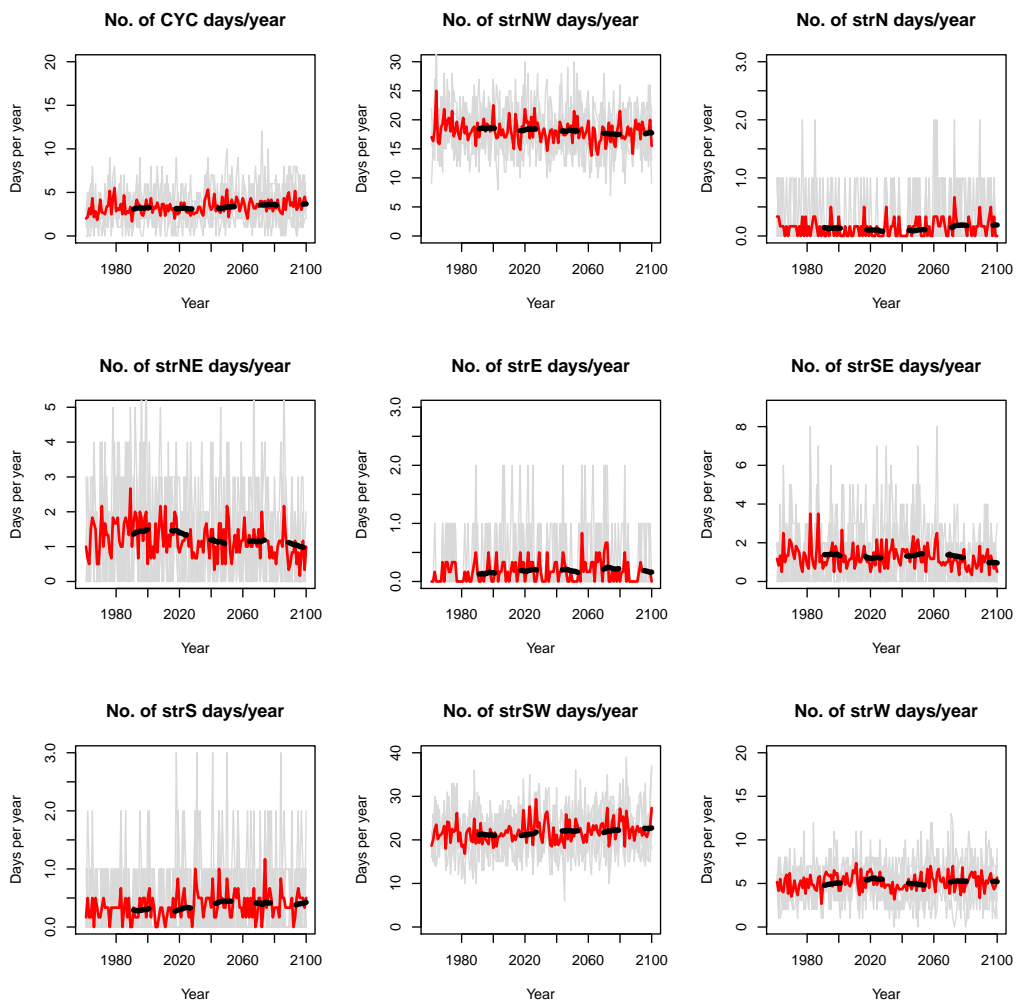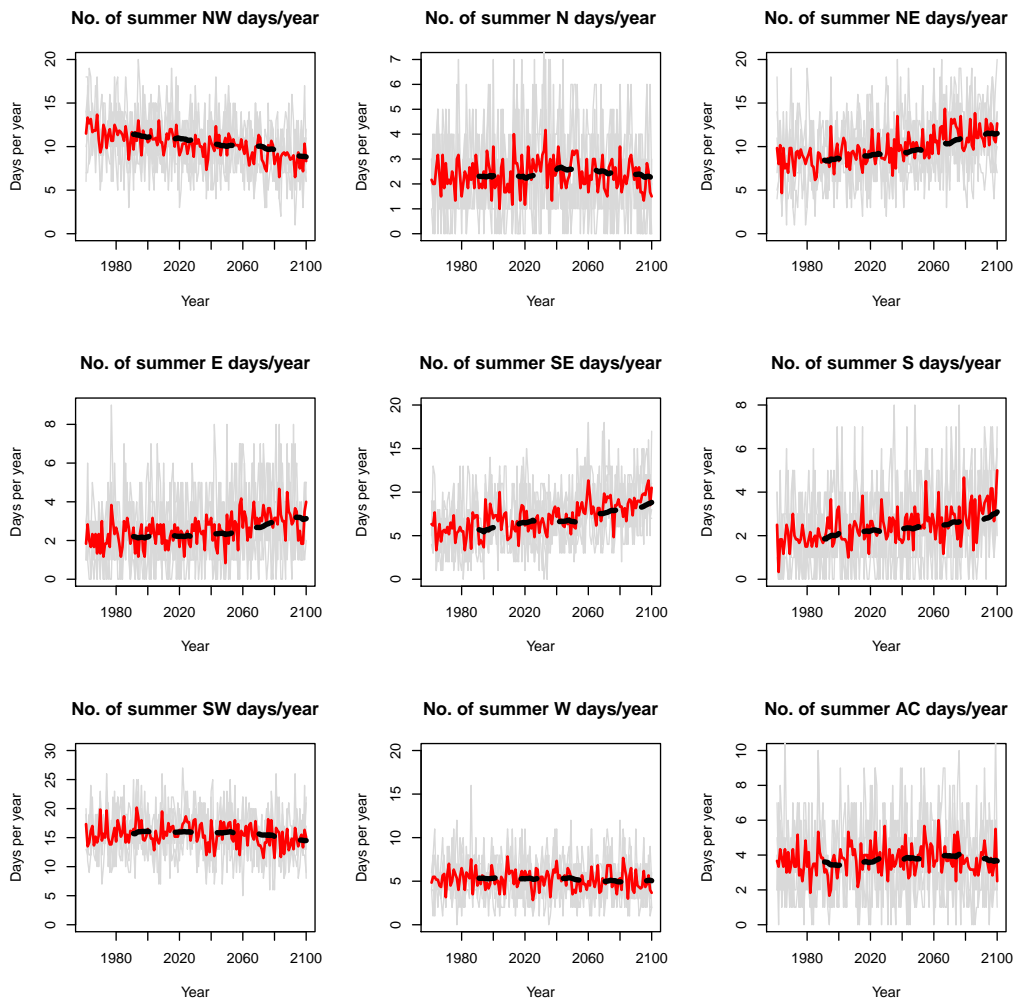
Figure D-2: Cont.

53

Figure D-3: Changes in summer frequencies of synoptic patterns Annual counts of each model are displayed as thin grey lines, the multi-model mean of the annual count is the bold red line, and the 30 year running mean of the multi-model mean is the black dashed line. (AC = Anticyclonic, CYC= Cyclonic, the "str" prefix indicates strong winds). (Cont. next page)

Figure D-3: Cont.

55

Figure D-4: Changes in autumn frequencies of synoptic patterns. Annual counts of each model are displayed as thin grey lines, the multi-model mean of the annual count is the bold red line, and the 30 year running mean of the multi-model mean is the black dashed line. (AC = Anticyclonic, CYC= Cyclonic, the "str" prefix indicates strong winds). (Cont. next page)
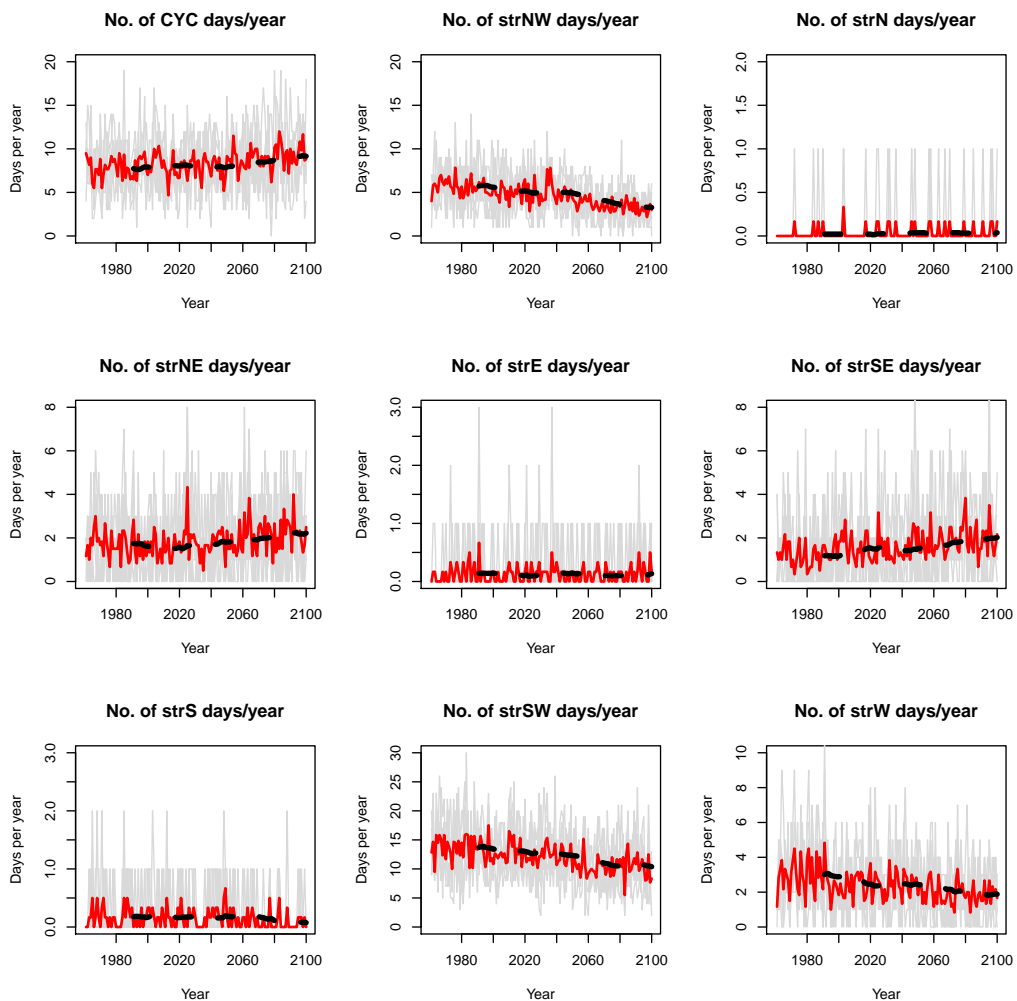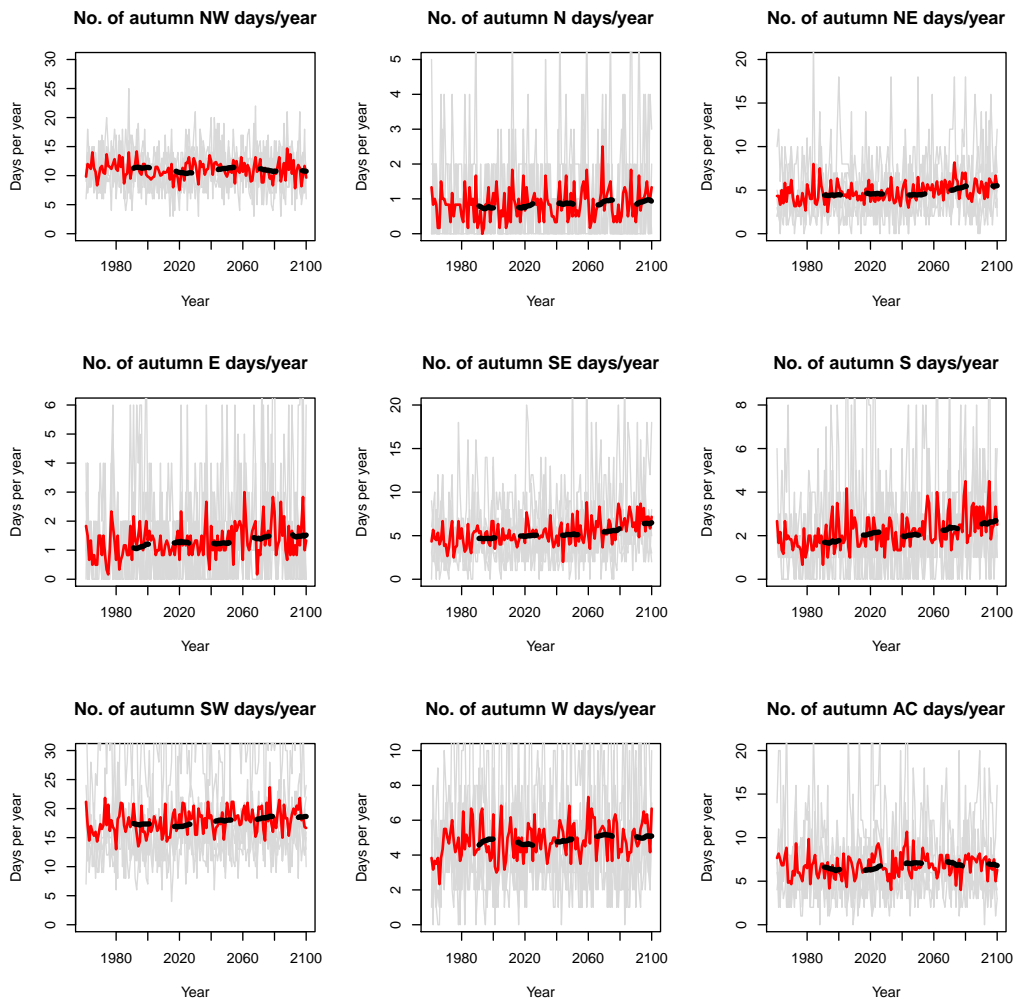
56

Figure D-4: Cont.

57

Figure D-5: Changes in winter frequencies of synoptic patterns. Annual counts of each model are displayed as thin grey lines, the multi-model mean of the annual count is the bold red line, and the 30 year running mean of the multi-model mean is the black dashed line. (AC = Anticyclonic, CYC= Cyclonic, the "str" prefix indicates strong winds). (Cont. next page)
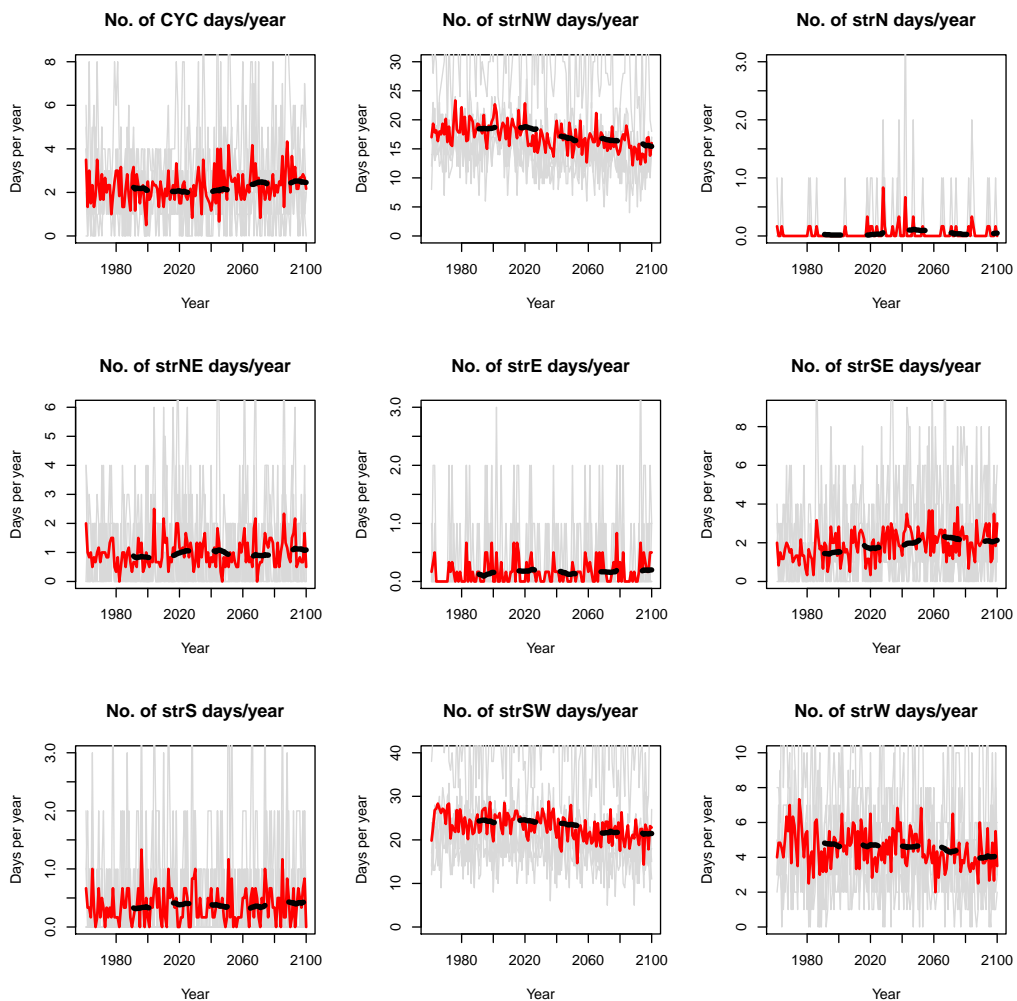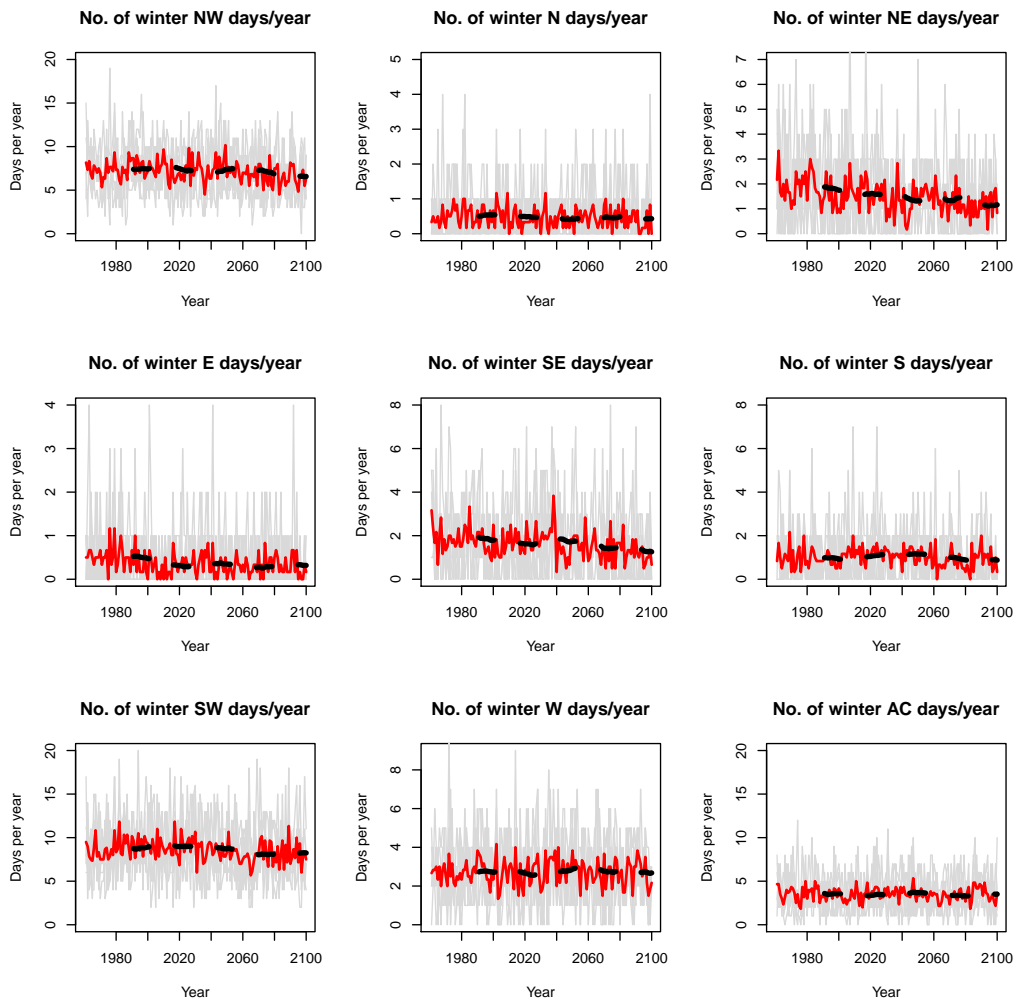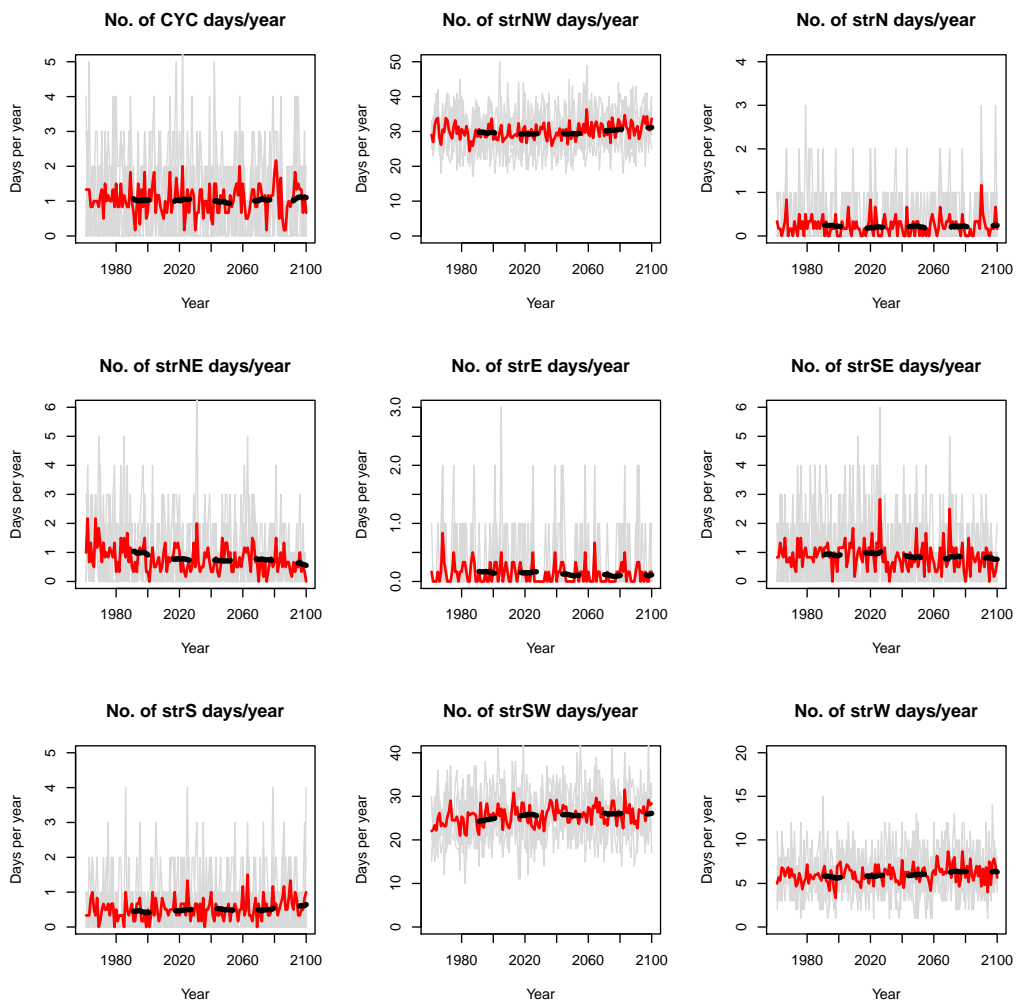
Figure D-5: Cont.

Appendix E: Weather variable data provided to Tasmanian Parks and Wildlife Service

Statistics of fire danger indices, dryness indicators, dry lightning potential environment and several fundamental meteorological parameters have been calculated and formatted for provision to the Tasmanian Parks and Wildlife Service for use in models for fire management such as the Bushfire Risk Assessment Model (BRAM). The statistics have been calculated for 46 regions which are defined as the "spheres of influence" surrounding the Bureau of Meteorology's weather stations. These regions together cover the entire state (Figure E-1).

For each calendar month the statistics of each parameter have been compiled for the 14 consecutive decades within the CFT analysis period. Parameters were analysed in two groups using methods similar to those described in Sections 2.1 and 3.1.

For FFDI, MFDI, MSDI, DF, temperature and wind speed, multi-model-maximum and multi-model-minimum 90th, 95th and 99th percentiles were calculated for each land grid cell in Tasmania and then averaged over each of the 46 regions. MF and relative humidity were analysed by the same method but for the 1st, 5th and 10th percentiles, as fire danger is inversely proportional to these parameters.

For MSDI threshold, antecendent rainfall threshold and DLPE, the area within each of the 46 regions meeting the criteria was calculated for each day. The multi-model-maximum and multi-model-minimum 90th, 95th and 99th percentiles of the daily area were then calculated for each region. Values are given as a percentage of the total land area of each region.

The statistics for each parameter are given in separate shapefiles. Each shape file contains 46 features corresponding to the weather station regions and 9 fields containing metadata for each feature and 1008 additional fields containing the statistics for each feature (12 months × 14 decades × 6 statistics). The naming convention for the fields is mmppyyyyMM where:

mm	-	Either "mx" for multi-model-maximum or "mi" for multi-model-minimum
pp	-	Percentile i.e. "01", "05", "10", "90", "95" or "99"
yyyy	-	First year of the decade over which the statistics have been calculated e.g. 1961
MM	-	Calendar month within the decade for which the statistics have been calculated e.g. 01

For example, for the shapefile containing the FFDI statistics, the field labelled mx99202101 contains the multi-model-maximum 99th percentile FFDI for all of the January days within the decade spanning 2021 to 2030, plotted
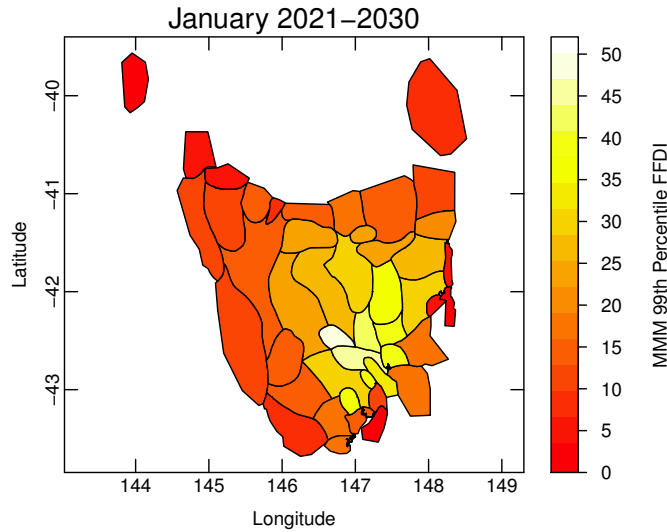
in Figure E-1.

Figure E-1: "Sphere of influence" regions for Tasmanian Bureau of Meteorology weather stations. Regions have been shaded according to the multi-model-maximum 99th percentile forest fire danger index for January during the decade of 2021–2030.

Shapefiles are provided as zip files, listed below, each containing .dbf, .prj, .shp and .shx files.

Filename	Variable
df.zip	Drought Factor
dryp.zip	Antecedent rainfall threshold
ffdi.zip	McArthur Forest Fire Danger Index
lpe0600.zip	Dry Lightning Potential Environment at 0600 UTC
lpe1200.zip	Dry Lightning Potential Environment at 1200 UTC
lpe1800.zip	Dry Lightning Potential Environment at 1800 UTC
lpe2400.zip	Dry Lightning Potential Environment at 2400 UTC
mf.zip	Moisture Factor
mfdi.zip	Moorland Fire Danger Index
rh.zip	Daily Minimum Relative Humidity
sdi.zip	Mount Soil Dryness Index
sdi_thresh.zip	Mount Soil Dryness Index Threshold
t.zip	Daily Maximum Temperature (degrees K)
wspd.zip	Daily Maximum Wind Speed (km/hour)

Appendix F: Weather variable data provided to Dr Jonathan Marsden-Smedley

Statistics of fire danger indices, dryness indicators, dry lightning potential environment and several fundamental meteorological parameters have been calculated and formatted for provision to Dr Jonathan Marsden-Smedley for application in research into the history of lightning fires in the TWWHA [*Marsden-Smedley*, 2016], commissioned as part of the TBCCRP. The statistics have been calculated as 10 km resolution gridded data for the TWWHA using the same method as applied to generate the data in Appendix A but without averaging over area.

For each calendar month the statistics of each parameter have been compiled for the four 20-year subperiods baseline (1980–2000), near-future (2010–2030), mid-century (2040–2060) and end-of-century (2080–2100).

For FFDI, MFDI, MSDI, temperature and wind speed, MMM 85th, 90th, 95th 99th, 99.5th and 99.9th percentiles were calculated for each land grid cell in the TWWHA. MF and relative humidity were analysed by the same method but for the 0.1st, 0.5th, 1st, 5th, 10th and 15th percentiles, as fire danger is inversely proportional to these parameters.

For MSDI threshold, antecedent rainfall threshold and DLPE, the statistic calculated was the number of days per calendar month that each grid cell was subject to conditions meeting the specified criteria.

Data were provided in Microsoft Excel format (.xlsx) with the naming convention twwha_<variable>_mmm_<period>_<month>.xlsx where:

<variable>	-	The variable for which statistics have been calculated:	
		"dryp"	Antecendent rainfall threshold
		"ffdi"	McArthur Forest Fire Danger Index
		"lpe"	Dry Lightning Potential Environment at 1200 UTC
		"mf"	Moisture Factor
		"mfdi"	Moorland Fire Danger Index
		"rh"	Daily Minimum Relative Humidity
		"sdi"	Mount Soil Dryness Index
		"sdi_thresh"	Mount Soil Dryness Index Threshold
		"t"	Daily Maximum Temperature (degrees K)
		"wspd"	Daily Maximum Wind Speed (km/hour)
<period>	-	20-year period of analysis, either "base", "near", "mid" or "end"	
<month>	-	Calendar month, ie, "jan", "feb", ...	

These data are also available in NetCDF format (.nc).

Further data available in NetCDF format

The same gridded statistics are available over the entire state of Tasmania for individual models as well as the MMM. In addition to monthly statistics, annual (July-June) and fire season (October–March) statistics (as in Appendix A) are also available. The naming convention for these further data is <variable>_<model>_<period>_<window>.nc where:

<variable>	-	The variable for which statistics have been calculated:
		"dryp" Antecendent rainfall threshold
		"ffdi" McArthur Forest Fire Danger Index
		"lpe" Dry Lightning Potential Environment at 1200 UTC
		"mf" Moisture Factor
		"mfdi" Moorland Fire Danger Index
		"rh" Daily Minimum Relative Humidity
		"sdi" Mount Soil Dryness Index
		"sdi_thresh" Mount Soil Dryness Index Threshold
		"t" Daily Maximum Temperature (degrees K)
		"wspd" Daily Maximum Wind Speed (km/hour)
<model>	-	CMIP3 model used as GDD, ie, "echam5", "gfdlcm20", "gfdlcm21","miroc", "Mk35", "ukhadcm3" or "mmm" (multi-model-mean)
<period>	-	20-year period of analysis, either "base", "near", "mid" or "end"
<window>	-	Calendar month, ie, "jan", "feb", ..., or "annual" or "oct-mar"

References

AFAC (2016), AFAC Independent Operational Review – A review of the management of the Tasmanian fires of January 2016, *Tech. rep.*, Australasian Fire and Emergency Services Authorities Council, Melbourne, Victoria.

Black, M., and D. J. Karoly (2016), Southern Australia's warmest October on record: The role of ENSO and climate change [in "Explaining Extremes of 2015 from a Climate Perspective"], *B. A. Met. Soc.*, *97*(12), S118–S121, doi:10.1175/BAMS-D-16-0124.1.

Corney, S. P., J. J. Katzfey, J. L. McGregor, M. R. Grose, J. C. Bennett, C. J. White, G. K. Holz, S. M. Gaynor, and N. L. Bindoff (2010), Climate Futures for Tasmania: climate modelling technical report, *Tech. rep.*, Antarctic Climate and Ecosystems Cooperative Research Centre, Hobart, Tasmania.

Deslandes, R., H. Richter, and T. Bannister (2008), The end-to-end severe thunderstorm forecasting system in Australia: overview and training issues, *Aust. Meteorol. Mag*, *57*(4), 329–343.

Dowdy, A., and G. A. Mills (2012), Atmospheric and fuel moisture characteristics associated with lightning-attributed fires, *J. Appl. Meteorol. Clim.*, *51*(11), 2025–2037, doi:10.1175/JAMC-D-11-0219.1.

Fox-Hughes, P. (2008), A fire danger climatology for Tasmania, *Aust. Meteorol. Mag*, *57*(2), 109–120.

Fox-Hughes, P., R. M. B. Harris, G. Lee, M. Grose, and N. L. Bindoff (2014), Future fire danger climatology for Tasmania, Australia, using a dynamically downscaled regional climate model, *Int. J. Wildland Fire*, *23*(3), 309–321, doi:10.1071/WF13126.

Fox-Hughes, P., R. M. B. Harris, G. Lee, J. Jabour, M. Grose, T. A. Remenyi, and N. L. Bindoff (2015), Climate Futures for Tasmania future fire danger: the summary and the technical report, *Tech. rep.*, Antarctic Climate and Ecosystems Cooperative Research Centre, Hobart, Tasmania.

Hope, P., G. Wang, E.-. P. Lim, H. H. Hendon, and J. M. Arblaster (2016), What caused the record-breaking heat across Australia in October 2015? [in "Explaining Extremes of 2015 from a Climate Perspective"], *B. A. Met. Soc.*, *97*(12), S122–S126, doi:10.1175/BAMS-D-16-0141.1.

Jones, D. A., W. Wang, and R. Fawcett (2009), High-quality spatial climate data-sets for australia, *Aust. Meteor. Oceanogr. J.*, *58*, 233–248.

Karoly, D. J., M. T. Black, M. R. Grose, and A. D. King (2016), The roles of climate change and El Niño in the record low rainfall in October 2015 in Tasmania, Australia [in "Explaining Extremes of 2015 from a Climate Perspective"], *B. A. Met. Soc.*, *97*(12), S127–S130, doi:10.1175/BAMS-D-16-0139.1.

Marsden-Smedley, J. B. (2009), Planned Burning in Tasmania: Operational Guidelines and Review of Current Knowledge, *Tech. rep.*, Tasmanian Parks and Wildlife Service, DPIPWE, Hobart, Tasmania.

Marsden-Smedley, J. B. (2016), Lightning fires and climate change in the Tasmanian Wilderness World Heritage Area, report prepared for: Tasmanian Climate Change Office Department of Premier and Cabinet, Tasmania.

Marsden-Smedley, J. B., and W. R. Catchpole (1995), Fire behaviour modelling in Tasmanian buttongrass moorlands. 2. Fire behaviour, *Int. J. Wildland Fire*, *5*(4), 215–228, doi:10.1071/WF9950215.

Marsden-Smedley, J. B., T. Rudman, A. Pyrke, and W. R. Catchpole (1999), Buttongrass moorland fire-behaviour prediction and management, *Tasforests*, *11*, 87–107.

Marsh, L. (1987), Fire weather forecasting in Tasmania, *Meteorological note 171*, Bureau of Meteorology, Melbourne, Australia.

McArthur, A. G. (1967), *Fire behaviour in eucalypt forests*, Forestry and Timber Bureau, Canberra.

Mount, A. B. (1972), The derivation and testing of a soil dryness index using run-off data, *Bulletin 4*, Forestry Commission of Tasmania.

Nguyen, H., A. Evans, C. Lucas, I. Smith, and B. Timbal (2013), The Hadley circulation in reanalyses: Climatology, variability, and change, *J. Clim.*, *26*(10), 3357–3376, doi:10.1175/JCLI-D-12-00224.1.

Nguyen, H., C. Lucas, A. Evans, B. Timbal, and L. Hanson (2015), Expansion of the southern hemisphere Hadley cell in response to greenhouse gas forcing, *J. Clim.*, *28*(20), 8067–8077, doi:10.1175/JCLI-D-15-0139.1.

Noble, I. R., A. M. Gill, and G. A. V. Bary (1980), McArthur's fire-danger meters expressed as equations, *Aust. J. Ecol.*, *5*(2), 201–203, doi:10.1111/j.1442-9993.1980.tb01243.x.

Press, A. K. (2016), Tasmanian Wilderness World Heritage Area bushfire and climate change research project, *Tech. rep.*, Tasmanian Government, Hobart, Australia.

Rorig, M. L., and S. A. Ferguson (1999), Characteristics of lightning and wildland fire ignition in the Pacific Northwest, *J. Appl. Meteorol.*, *38*(11), 1565–1575, doi:10.1175/1520-0450(1999)038<1565:COLAWF>2.0.CO;2.

Seidel, D. J., Q. Fu, W. J. Randel, and T. J. Reichler (2008), Widening of the tropical belt in a changing climate, *Nat. Geosci.*, *1*(1), 21–24, doi:10.1038/ngeo.2007.38.

Styger, J. K., and J. B. Kirkpatrick (2015), Less than 50 millimetres of rainfall in the previous month predicts fire in Tasmanian rainforest, *Papers and Proceedings of the Royal Society of Tasmania*, *149*, 1–5.

Styger, J. K., J. B. Marsden-Smedley, and J. B. Kirkpatrick (2018), Changes in lightning fire incidence in the tasmanian wilderness world heritage area, 1980-2016, *Fire*, *1*(3), 38, doi:10.3390/fire1030038.